Numerical computation of the chemical dissociation and relaxation phenomena behind a detached strong shock

Jean-Antoine Desideri, Loula Fatima Fezoui, Nathalie Glinsky

UNITÉ DE RECHERCHE
INRIA-SOPHIA ANTIPOLIS

Institut National
de Recherche
en Informatique
et en Automatique

Domaine de Voluceau
Rocquencourt
B.P.105
78153 Le Chesnay Cedex
France
Tél. (1) 39 63 55 11

Rapports de Recherche

N° 774

NUMERICAL COMPUTATION OF THE CHEMICAL DISSOCIATION AND RELAXATION PHENOMENA BEHIND A DETACHED STRONG SHOCK

Jean-Antoine DESIDERI
Loula FEZOUI
Nathalie GLINSKY

DECEMBRE 1987

NUMERICAL COMPUTATION OF THE CHEMICAL DISSOCIATION AND RELAXATION PHENOMENA BEHIND A DETACHED STRONG SHOCK

Simulation numérique des phénomènes de dissociation chimique et de relaxation derrière un choc détaché

Jean-Antoine DESIDERI
Loula FEZOUI
Nathalie GLINSKY

INRIA Sophia-Antipolis
2004, Route des Lucioles
Parc de Sophia-Antipolis 1 et 2
06560 VALBONNE

Abstract

A one-dimensionnal stiff problem modeling the chemical dissociation and relaxation phenomena behind a strong detached shock is solved numerically by a space-marching technique and two time integration methods (explicit/implicit). Characteristic time/length-scales are identified. The efficiency of the linearized Euler implicit method is demonstrated.

Résumé

On résoud numériquement un problème monodimensionnel qui modélise les phénomènes de dissociation chimique et de relaxation derrière un choc fort détaché par une méthode d'avancement en espace, et deux méthodes d'intégration en temps (explicite/implicite). On identifie les échelles caractéristiques de temps et de longueur. On démontre l'efficacité de la méthode d'Euler implicite linéarisée.

NOTATIONS

ρ	density (kg/m^3)
V	velocity (m/s)
p	pressure (N/m^2)
C	local sound velocity $C = \sqrt{\frac{\gamma p}{\rho}}$
M_∞	Mach number at the entry in the atmosphere
T	temperature (K)
t	time
Y	mass fraction
q	concentration $(mol./kg)$
h	enthalpy by unit mass (J/kg)
H	total enthalpy by unit mass (J/kg)
h^0	formation enthalpy by unit mass (J/kg)
m	mass
$\overline{m}$	molar mass
$\mathcal{R}$	universal gas constant 8.32 J/K
R	specific gas constant $R = \frac{\mathcal{R}}{m}$ $(J/K.kg)$
γ	specific heat ratio $\gamma = \frac{C_p}{C_v}$
$\mathcal{N}$	Avogadro constant
$\mathcal{V}$	control volume

Subscripts
i refers to species i
j refers to abscissa x_j

Superscripts

n	time level

Table of Contents

I. INTRODUCTION

The atmospheric reentry of a space vehicle such as the european shuttle HERMES occurs at an altitude of approximately 60 km and a hypersonic flight Mach number

$$M_\infty = \frac{V_\infty}{C_\infty}$$

(V_∞: relative air/engine velocity; C_∞: local sound speed) that may range from 15 to 25. As a result, a strong shock in front of the vehicule causes important variations of the physical values of the air flow.

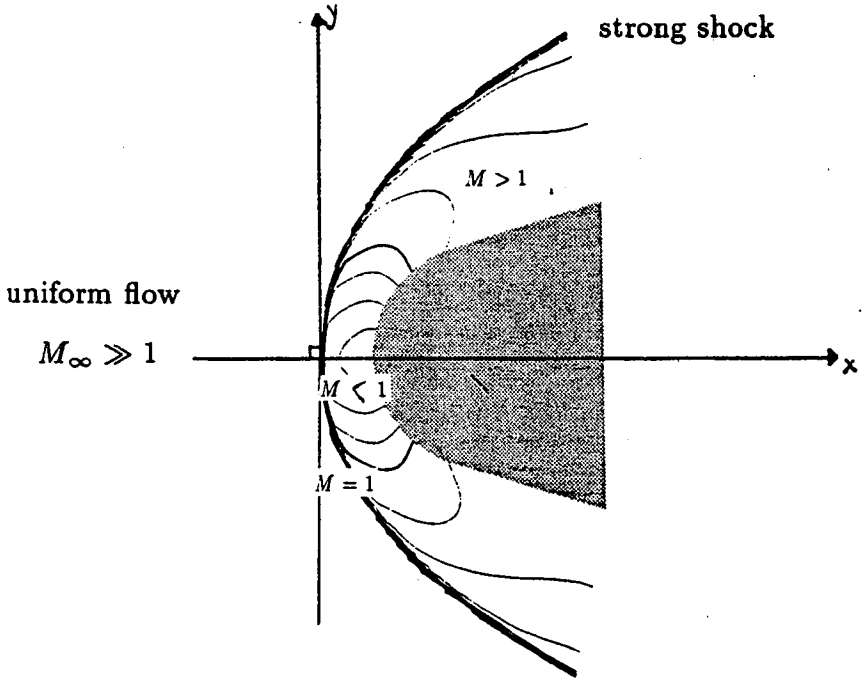

Upstream the shock, the flow is uniform, the temperature is low and air is a mixture of uniform composition, which main compounds are nitrogen (79%) and oxygen (21%). Through the shock, the temperature increases extensively. For a steady perfect gas the static temperature is constant along a streamline and given by

$$\frac{T_s}{T_\infty} = 1 + \frac{\gamma - 1}{2} M_\infty^2$$

where γ is the ratio of specific heats ($\gamma = 1.4$ for air). This temperature is also the temperature at the stagnation point. For example, with $T_\infty = 231$ K and $M_\infty = 25$

we obtain $T_s \sim 29000$ K. Then obviously, the hypothesis of inert gas is completely inaccurate, as we can see on Figure 1 where the temperatures at the vehicule nose for both inert and reactive gas are compared (taken from [1]).

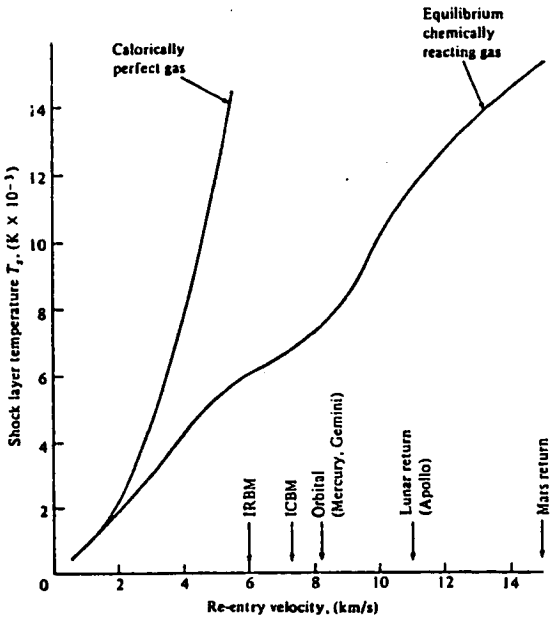

Figure 13.1 Temperature behind a normal shock versus velocity for air at a standard altitude of 52 km. Comparison between calorically perfect and equilibrium gas results.

Long before this temperature T_s is reached, the air molecules dissociate causing an important fall of the temperature, since the dissociaton reactions are endothermic.

For these reasons, the simulation of hypersonic flow to be pertinent, in particular with respect to the temperature field computation - a crucial issue to the designer - must involve some evaluation of the chemical dissociation phenomena. While other authors [6] have developed simple, that is algebraic, equilibrium models to complete the governing flow equations (Euler equations), here, we experiment some classical numerical methods to simulate a complex set of chemical reactions (non-equilibrium chemistry) in a simplified model flow. We consider a one-dimensional relaxation process behind a strong normal shock, letting density and velocity be fixed and given by the Rankine-Hugoniot jump conditions. Other authors have employed this approach to evaluate the various components of the physical phenomenon [13]. Our aim is identify the difficulties and propose methods to compute numerically such problems.

In Chapter I, the employed chemical reactional scheme is defined precisely.

In chapter II, numerical methods for both the stiff ordinary differential equations governing the spatial Cauchy (steady-state) problem, and the time/space partial differential equations expressing the convection of species are tested. The linearized Euler implicit method is found very stable and efficient even in the presence of the source term causing increased stiffness.

II. PHYSICAL MODEL

1. Reactional scheme

For normal temperature conditions, air is composed of 79% nitrogen and 21% oxygen. However, it is not an inert gas, and its composition highly depends on the temperature. When (T $\geq$ 2500)), diatomic species N_2 and O_2 react: dissociations, recombinaisons and ionisations occur transforming the initial composition in a mixture of many compounds: N_2, O_2, NO, N, O, NO^+, O^+, N^+, O^-, N^-, e^- ..... in proportions which are fonctions of the temperature [1].

1.1. *Dissociation equations*

We employ a model developed in the United States during the 1970's [3]. The model is relatively simple and has been tested to give reasonable equilibrium compositions in the temperature range of concern. Ionization is neglected. Five species are retained O, N, NO, O_2 and N_2 subscripted from 1 to 5 in this order. The chemical equations studied are (Zel'dovich, [5]):

$$\begin{cases} O_2 + X \rightleftharpoons O + O + X & (1) \\ N_2 + X \rightleftharpoons N + N + X & (2) \\ NO + X \rightleftharpoons N + O + X & (3) \\ NO + O \rightleftharpoons O_2 + N & (4) \\ N_2 + O \rightleftharpoons NO + N & (5) \\ N_2 + O_2 \rightleftharpoons NO + NO & (6) \end{cases}$$

X represents a collision factor which can be any species of the five present. Hence these equations represent a total of 18 reactions, dissociation reactions ((1),(2),(3)) and bimolecular exchange reactions ((4),(5)). The latter are the most important for the formation of nitric oxide NO in air.

Note that the reaction in (6) can be obtained by adding the reactions in (4) and (5). However, contrasting with the equilibrium composition, in a nonequilibrium phenomenon, the chemical equations do not have to be independent.

The species production from N_2 and O_2 is endothermic, the reactions will thus

result in a high temperature decrease.

1.2. *Conservation equations*

The composition of the mixture is defined by the values of the mass fractions denoted $Y_i = \frac{m_i}{m}$ where m_i is the mass of species i contained in a control volume $\mathcal{V}$ and m is the mass of the mixture for this volume.

1.2.1. *Mass conservation*

By definition of the mass fractions :

$$\sum_{i=1}^{5} Y_i = 1 \tag{7}$$

1.2.2. *Species conservation*

If molecular diffusion is neglected, the number of atoms of nitrogen M_N present in the form of N_2, NO and N and O in a fluid element that we follow in its movement is constant with the time and the same is true for the number of atoms of oxygen M_O. Hence the ratio $\frac{M_N}{M_O}$ is uniform in space and time, and is equal to 79/21 as in the inert freestream:

$$M_O = \frac{2\mathcal{N}Y_{O_2}m}{\overline{m}_{O_2}} + \frac{\mathcal{N}Y_O m}{\overline{m}_O} + \frac{\mathcal{N}Y_{NO}m}{\overline{m}_{NO}}$$

$$M_N = \frac{2\mathcal{N}Y_{N_2}m}{\overline{m}_{N_2}} + \frac{\mathcal{N}Y_N m}{\overline{m}_N} + \frac{\mathcal{N}Y_{NO}m}{\overline{m}_{NO}}$$

This gives us the species conservation equation:

$$\frac{\frac{Y_{N_2}}{\overline{m}_N} + \frac{Y_N}{\overline{m}_N} + \frac{Y_{NO}}{\overline{m}_{NO}}}{\frac{Y_{O_2}}{\overline{m}_O} + \frac{Y_O}{\overline{m}_O} + \frac{Y_{NO}}{\overline{m}_{NO}}} = \frac{79}{21} \tag{8}$$

1.3. *Expression of energy*

The fluid considered is a mixture of perfect gases. The total energy (per unit of volume) of the mixture is the sum of the energies of the individual species:

$$E = \sum_{i=1}^{5} E_i \tag{9}$$

where

$$E_i = \frac{1}{2}\rho_i V^2 + \rho_i \varepsilon_i \tag{10}$$

where ε_i is the internal energy per unit of mass of the species i and ρ_i is the density of the species i.

We define the enthalpy per unit of mass of species i :

$$h_i = \varepsilon_i + \frac{p_i}{\rho_i} \tag{11}$$

where p_i is the partial pressure.

According to the definition of the enthalpy

$$h_i(T) = h_i(T_0) + \int_{T_0}^{T} C_{p_i} dT \tag{12}$$

where T_0 is a reference temperature ($T_0 = 298$ K); C_{p_i} is the specific heat per unit mass at constant pressure of species i, and is assumed to be constant (calorifically perfect gases):

$$C_p = \frac{7}{2}R \; for \; a \; diatomic \; species$$

$$C_p = \frac{5}{2}R \; for \; a \; monoatomic \; species$$

Also, $h_i(T_0) = h_i^0$ is the formation enthalpy per unit of mass of species i, and its value depends on the temperature T_0.

Injecting (11) and (12) in equation (10) gives:

$$E_i = \frac{1}{2}\rho_i V^2 + \rho_i h_i^0 + \rho_i C_{p_i}(T - T_0) - p_i \tag{13}$$

The density of species i is given by:

$$\rho_i = \rho Y_i \tag{14}$$

Each gas being perfect, it verifies the perfect gas law

$$p_i = \rho_i \frac{\mathcal{R}}{m_i} T \tag{15}$$

and the Dalton's law gives us the total pressure in terms of the partial pressures:

$$p = \sum_{i=1}^{5} p_i \tag{16}$$

This gives us the state equation for the mixture:

$$p = \rho \mathcal{R} T \sum_{i=1}^{5} \frac{Y_i}{m_i}$$

Combining (13),(14),(15),(16), the total energy of the mixture is expressed as follows:

$$E = \frac{1}{2}\rho V^2 + \rho \sum_{i=1}^{5} Y_i h_i^0 + \rho(\sum_{i=1}^{5} Y_i C_{p_i})(T - T_0) - \rho \mathcal{R} T \sum_{i=1}^{5} \frac{Y_i}{m_i} \tag{17}$$

1.4. *Enthalpy conservation equation*

The energy conservation equation is written in a general form in possibly several dimensions (last Euler equation)

$$\frac{\partial}{\partial t} E + div\big((E + p)\vec{V}\big) = 0 \tag{18}$$

We introduce the total enthalpy per unit of mass

$$H = \frac{E + p}{\rho} = \frac{1}{2}V^2 + h_i \tag{19}$$

or as well

$$H = \frac{1}{2}V^2 + \sum_{i=1}^{5} Y_i h_i^0 + (T - T_0) \sum_{i=1}^{5} Y_i C_{p_i} \tag{20}$$

The conservation equation (18) becomes:

$$\frac{\partial}{\partial t} E + div(\rho \vec{V} H) = 0 \tag{21}$$

It follows that at the steady state,

$$div(\rho \vec{V} H) = 0$$

or equivalently

$$div(\rho \vec{V}) H + (\rho \vec{V}).\vec{\nabla} H = 0$$

But the satisfaction of the continuity equation implies that $div(\rho \vec{V}) = 0$, and therefore:

$$\vec{V}.\vec{\nabla} H = 0 \tag{22}$$

We conclude that H is a constant along a streamline. If all the streamlines emanate from the same uniform flow, H is constant everywhere ("iso-energetic flow").

$$H = constant \tag{23}$$

This equation is used with the expression of energy given in the previous section to calculate the temperature from the mass fractions.

1.5. *Evolution equations*

1.5.1. *Mass conservation*

The mass convection equation for species i is expressed by

$$\frac{\partial}{\partial t}(\rho Y_i) + div(\rho Y_i \vec{V}) = \Omega_i \tag{25}$$

where Ω_i is the mass production rate of species i (production term). Here we recall the form of these terms in the case of a simple reaction $A \rightleftharpoons B$. When more than one reaction is considered, several terms of this type are added up to form each Ω_i. (for more details, see [1]).

1.5.1.1. *Case of a simple reversible reaction*

In the case of an irreversible reaction $A \rightarrow B$, the equation of mass conservation of the species A reads:

$$\frac{\partial}{\partial t}(\rho Y_A) + div(\rho Y_A \vec{V}) = -(\frac{\rho Y_A}{m}) K_A e^{-\frac{E_A}{RT}} f(T) \tag{26}$$

E_A is the activation energy of the reaction, and $K_A f(T)$ the Arrhenius factor, in which K_A is a constant, and $f(T)$ is a function of temperature, generally expressed as a polynomial curvefit of experimental data. The term in $e^{-\frac{E}{RT}}$ result from the Arrhenius's law which express the high dependance on temperature of the reaction production rate. If we consider now the reversible reaction $A \rightleftharpoons B$, the mass variation of the species A becomes:

$$\Omega_A = K'_A \left(\frac{\rho(1 - Y_A)}{m}\right) e^{-\frac{E'_A}{RT}} g(T) - K_A \left(\frac{\rho Y_A}{m}\right) e^{-\frac{E_A}{RT}} f(T) \tag{27}$$

where K'_A, E'_A and g are the values of the chemical constants of the reverse reaction.

2. Frozen Aerodynamic Flowfield

We recall here the jump conditions [1], or Rankine-Hugoniot relations, that give the flow properties behind a normal shock denoted by unsubscripted symbols, in terms of the freestream Mach number M_∞ and the ratio of specific heats γ:

$$\frac{p}{p_\infty} = \frac{2\gamma}{\gamma+1} M_\infty^2 - \frac{\gamma-1}{\gamma+1} \tag{38}$$

$$\frac{\rho}{\rho_\infty} = \frac{1}{\frac{2}{\gamma+1}\cdot\frac{1}{M_\infty^2} + \frac{\gamma-1}{\gamma+1}} \tag{39}$$

$$\frac{T}{T_\infty} = \frac{p}{p_\infty}\cdot\frac{\rho_\infty}{\rho} \tag{40}$$

$$\frac{V}{V_\infty} = \frac{\rho_\infty}{\rho} \tag{41}$$

For practical applications, these ratios are evaluated for $M_\infty = 15$, 20 and 25, and the standard atmosphere at an altitude of 60 km, so that:
$p_\infty = 10\ N/m^2$, $\rho_\infty = 1.5\ 10^{-4}\ kg/m^3$, $T_\infty = 231\ K$.
This gives:

Mach	V_∞	V	p	ρ	T
25	7637.6	1283.1	7290	$8.92.10^{-4}$	28291
20	6110.2	1032.1	4665	$8.88.10^{-4}$	18185
15	4582.6	781.1	2623	$8.80.10^{-4}$	10324

Table I

In our one-dimensional model problem, the variables ρ and V are maintained constant over the domain and equal to these values.

3. Summary of the governing equations

The system to be solved has the following form:

$$\begin{cases} \dfrac{\partial}{\partial t}(\rho Y_i) + div(\rho Y_i \vec{V}) = \Omega_i \\ T = f(Y_i, \rho) \end{cases} \tag{42}$$

Using the conservation equations (7)-(8), three such convection equations are written, the mass fractions of N_2 and O_2 being calculated from the rest. The temperature is obtained from the mass fractions via the total enthalpy conservation equation (23).

Thus, in one dimension the system reduces to:

$$\begin{cases} (\rho Y_i)_t + (\rho Y_i V)_x = \Omega_i \quad i = 1...3 \\ Y_4 = \dfrac{24}{103} - Y_1 - \dfrac{8}{15} Y_3 \\ Y_5 = \dfrac{79}{103} - Y_2 - \dfrac{7}{15} Y_3 \\ T = \dfrac{H_\infty - \dfrac{1}{2}V^2 - \sum_{i=1}^{5} Y_i h_i^0}{\sum_{i=1}^{5} Y_i C_{p_i}} + T_0 \end{cases} \tag{43}$$

in which T_0 is the reference temperature $T_0 = 298\ K$.

Initially ($t = 0$), the following composition of air is enforced:

$$\begin{cases} Y_1 = Y_2 = Y_3 = 0 \\ Y_4 = \dfrac{24}{103} \\ Y_5 = \dfrac{79}{103} \\ T: \text{ temperature behind the shock (40)} \end{cases}$$

The variables ρ and V assumed fixed values. The system is hyperbolic in both time and space.

The source terms Ω_i are calculated from the table II. They are of the type $\Omega_i(Y_1, Y_2, Y_3, Y_4, Y_5, T, \rho)$. Finally, the following values are used for the formation enthalpies [2]:

$$\begin{cases} h_1^0 = \dfrac{249.2}{16}.10^6\ J/kg \\ h_2^0 = \dfrac{472.7}{14}.10^6\ J/kg \\ h_3^0 = \dfrac{90.3}{30}.10^6\ J/kg \end{cases}$$

h_4^0 and h_5^0 are null since the species O_2 and N_2 are already formed.

Table 1 Reactions considered and their equilibrium constants. The subscript e in this table designates equilibrium condition; temperature T is in °K

n	Reaction	Equilibrium Constant K_n
1	$O_2 + X \rightleftharpoons O + O + X$	$K_1 \equiv \rho(q_1^2/q_4)_e = (28.756 - 2.624\times10^{-3}\,T + 9.894\times10^{-8}\,T^2)\exp(-59500\,T^{-1})$
2	$N_2 + X \rightleftharpoons N + N + X$	$K_2 \equiv \rho(q_2^2/q_5)_e = (21.321 - 1.23\times10^{-3}\,T + 1.1091\times10^{-7}\,T^2)\exp(-113000\,T^{-1})$
3	$NO + X \rightleftharpoons N + O + X$	$K_3 \equiv \rho(q_1q_2/q_3)_e = (6.1007 - 5.105\times10^{-4}\,T + 2.957\times10^{-8}\,T^2)\exp(-75500\,T^{-1})$
4	$NO + O \rightleftharpoons O_2 + N$	$K_4 \equiv (q_4q_2/q_3q_1)_e = K_3/K_1$
5	$N_2 + O \rightleftharpoons NO + N$	$K_5 \equiv (q_2q_3/q_1q_5)_e = K_2/K_3$
6	$N_2 + O_2 \rightleftharpoons NO + NO$	$K_6 \equiv (q_3^2/q_4q_5)_e = (K_1K_2/K_3^2)$

Table 2 Species production rates; density ρ in this table is expressed in g/cm^3

n	ω_n
1	$(\partial q_1/\partial t)_1 + (\partial q_1/\partial t)_3 + (\partial q_1/\partial t)_4 - (\partial q_1/\partial t)_5$
2	$(\partial q_2/\partial t)_2 + (\partial q_1/\partial t)_3 - (\partial q_1/\partial t)_4 + (\partial q_1/\partial t)_5$
3	$-(\partial q_1/\partial t)_3 + (\partial q_1/\partial t)_4 + (\partial q_1/\partial t)_5 + (\partial q_3/\partial t)_6$

Definitions of Terms $(\partial q_m/\partial t)_m$

$(\partial q_1/\partial t)_1 \equiv 2\kappa_1\rho(K_1q_4 - \rho q_1^2)$	$(\partial q_1/\partial t)_5 \equiv \kappa_5\rho(K_5q_1q_5 - q_2q_3)$
$(\partial q_1/\partial t)_3 \equiv \kappa_3\rho(K_3q_2 - \rho q_1q_2)$	$(\partial q_2/\partial t)_2 \equiv 2\kappa_2\rho(K_2q_5 - \rho q_2^2)$
$(\partial q_1/\partial t)_4 \equiv -\kappa_4\rho(K_4q_1q_3 - q_2q_4)$	$(\partial q_3/\partial t)_6 \equiv 2\kappa_6\rho(K_6q_4q_5 - q_3^2)$

Table 3 Reverse rate coefficients k_{nm} for three-body reactions $\kappa_n = \sum_{m=1}^{5} k_{nm}q_m$, $n = 1,3$

n	m	k_{nm}
1	1	$4.14\times10^{18}\,T^{-1}\exp(-171.5\,T^{-1})$
1	2	k_{11}
1	3	$k_{11}/3$
1	4	$k_{11}/3$
1	5	$k_{11}/3$
2	1	$9.0\times10^{14}\exp(500\,T^{-1})$
2	2	k_{21}
2	3	$k_{21}/3$
2	4	$k_{21}/3$
2	5	$k_{21}/3$
3	1	$1.28\times10^{17}\,T^{-0.5}$
3	2	k_{31}
3	3	$k_{31}/2$
3	4	$k_{31}/2$
3	5	$k_{31}/2$

Here n = 1,2,3 refer to reactions indicated in Table 1, and m = 1 - 5 indicate species acting as the third body of reaction. Temperature T in this table is in °K.

Table 4 Reverse rate coefficients κ_n for binary reactions n = 4,5,6; temperature T in this table is in °K

n	κ_n
4	$1.015\times10^{10}\,T\exp(-3096\,T^{-1})$
5	1.6×10^{13}
6	0.0

Table II (taken from [3])

III. NUMERICAL SOLUTION

In this chapter, numerical methods for the solution of (43) are developed and tested. Since the simplified system is hyperbolic in both time and space, the steady system can be marched spatially. This is done in section 1, and this allows us to identify the principal scales involved in the model. However, in view of future applications in which the chemistry equations are coupled with the flow equations and to be solved in subsonic regions where the complete system is elliptic, efficient methods applicable to the time/space formulation are also examined in section 2.

1. Stationary problem - O.D.E

The stationary problem is hyperbolic in space and can therefore be marched:

$$\begin{cases} \dfrac{\partial}{\partial x}(\rho Y_i V) = \Omega_i \quad i = 1..3 \\ Y_4 = \dfrac{24}{103} - Y_1 - \dfrac{8}{15}Y_3 \\ Y_5 = \dfrac{79}{103} - Y_2 - \dfrac{7}{15}Y_3 \\ T = \dfrac{H_\infty - \frac{1}{2}V^2 - \sum_{i=1}^{3} Y_i h_i^0}{\sum_{i=1}^{5} Y_i C_{p_i}} + T_0 \end{cases} \tag{44}$$

For this we employ a nonlinearly 4th-order Runge-Kutta method.

1.1. *Runge-Kutta method*

We define

$$W = \begin{pmatrix} \rho Y_1 \\ \rho Y_2 \\ \rho Y_3 \end{pmatrix}$$

and rewrite the system as the following 1st-order vector ordinary differential equation

$$\frac{\partial}{\partial x}(VW) = \Omega(W, T, \rho)$$

or

$$\frac{\partial}{\partial x}W = G(W,T,\rho) = \frac{\Omega(W,T,\rho)}{V}$$

The 4-stage explicit method is defined as follows

$$\begin{cases} W_{j+1} = W_j + \dfrac{h}{6}(K_1 + 2K_2 + 2K_3 + K_4) \\ where \\ K_1 = G(W_j, T_j, \rho) \\ K_2 = G(W_j + \dfrac{h}{2}K_1, T_j, \rho) \\ K_3 = G(W_j + \dfrac{h}{2}K_2, T_j, \rho) \\ K_4 = G(W_j + hK_3, T_j, \rho) \end{cases}$$

Once the three components of W_{j+1} are determined, $Y_{4_{j+1}}$, $Y_{5_{j+1}}$ and T_{j+1} are computed from (44).
This method was selected since it is fourth-order accurate for a general nonlinear O.D.E.

1.2. *Numerical results*

The essential result is that the problem is stiff and highly depends on the temperature and then the Mach number (table I).
The source terms

$$F_i(Y_i,T,\rho) = \frac{\partial}{\partial x}Y_i = \frac{\Omega_i(Y_i,T,\rho)}{\rho V}$$

are represented on figures 1, 2 and 3 for M_∞=25, 20 and 15 respectively.
We can see that for $M_\infty = 25$ (figure 1), the source term F_2,which initial value is 8000, diminishes of a factor 10 over a distance of 0.1 mm. The variation is more moderate for $M_\infty = 20$ (figure 2) since the term F_2 diminishes of a factor 10 over a distance of 1 mm, the initial value being 500. The variation is even more moderate for $M_\infty = 15$ (figure 3), since F_1 diminishes of a factor 10 over a distance of 1 cm , the initial value being 45 .

Because the problem is very nonlinear and stiff, it was not possible to employ the same step h without precaution. Unadmissible values are computed (mass fractions outside the range [0,1] or negative temperatures) when at all computed. To circumvent this difficulty a simple procedure to control the stepsize was divised.
Note that if W_j is admissible, then so is W_{j+1} provided h is small enough. Thus, anytime the prediction for W_{j+1} was found to be unadmissible, the prediction was

respected, h was cut in two, and a new prediction was made. Also in order to avoid introducing induly many subdivisions, an attempt to double the stepsize was made after ten succesive iterations were performed with the same h.
The corresponding adapted meshes are shown on figure 4. The initial stepsize is 10^{-6} m. The maximum stepsize was found to be of the ordre of 10^{-2} m for $M_\infty = 25$ *and* 20 and of the order of 10^{-1} m for $M_\infty = 15$. This method allows us to use only 150 points of discretization.

The solutions (figures 5,6 and 7) indicate the dependence of the "effective relaxation lengths" and the temperature on the Mach number. We can see that it takes some 10 cm to the mass fractions to converge or "relax" to the equilibrium values. The equilibrium state can be calculated directly by applying the mass action law (cf. table I.1).

For M_∞=25, the temperatures at equilibrium are between 6137 K and 7919 K, and that is more than 20000 K less than the value at $x = 0$.
To illustrate this, we can calculate caracteristic reaction and relaxation lengths: δ and δ'. δ as the distance necessary to Y_{N_2} to be reduced by a half and δ' as the distance necessary to Y_{NO} to reach its maximum. For a stiff problem $\delta \ll \delta'$.

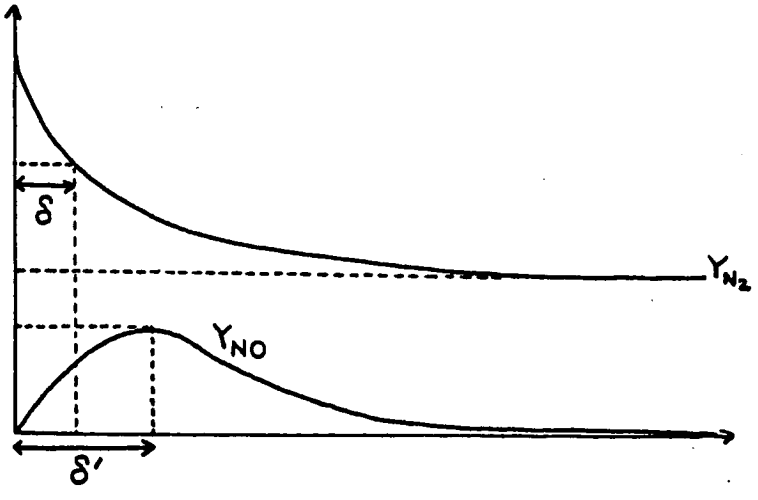

The approximate values of δ and δ' in m are:

M_∞	δ	δ'
25	1.10^{-4}	8.10^{-4}
20	5.10^{-4}	3.10^{-3}
15	7.10^{-3}	3.10^{-2}

Table III

2. Solution of the time-dependant problem by an explicit method

In view of extensions to 2-D Euler flow simulations in regions where the PDE's are not spatially hyperbolic it is important to also develop solution methods for the time-dependant problem (43).

2.1. *The Finite Volume Method*

The finite volume method corresponds to an integral form discretisation of the conservation law. With the same notations as employed for the stationary case, the partial-differential of (43) is written as follows:

$$W_t + (VW)_x = \Omega \tag{45}$$

which is of the following conservative form:

$$W_t + F(W)_x = \Omega \tag{46}$$

$F(W)$ is the flux function. In our case, F is linear $F(W) = VW$, but Ω is the source term and is highly nonlinear.
The domain is discretized in $N+1$ points x_j and each interval is divided in two to form a cell:

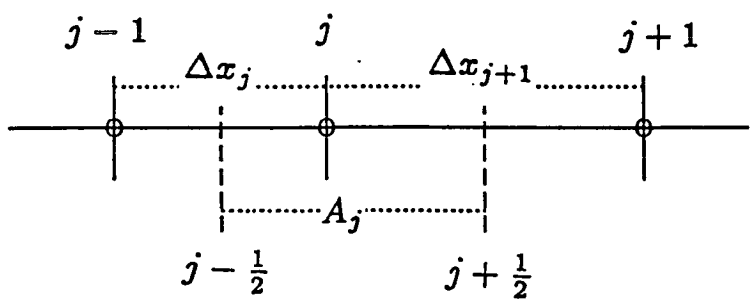

cell C_j

$\Delta x_j = x_j - x_{j-1}$ A_j: cell area $A_j = \frac{\Delta x_j + \Delta x_{j+1}}{2}$

$$F(W) = A(W)W$$

where $A(W) = F'(W)$ is the Jacobian.
In order to construct an upwind scheme particularly adapted to a convection equation admitting a preferential direction, we apply flux splitting. For this, A is diagonalized:

$$A = X^{-1}\Lambda X$$

where

$$A^- = X^{-1}\Lambda^- X \quad A^+ = X^{-1}\Lambda^+ X$$

and split into positive and negative parts

$$A(W) = A^+(W) + A^-(W)$$

Equation (48) is discretized in time by application of the Euler's scheme

$$\frac{W^{n+1} - W^n}{\Delta t} + F(W)_x = \Omega \tag{47}$$

in which Δt: time step, and W^n and W^{n+1} represent the vector W at times $n\Delta t$ and $(n+1)\Delta t$.
To discretize spatially, (49) is integrated over the cell C_j. This gives

$$A_j \left(\frac{W_j^{n+1} - W_j^n}{\Delta t} \right) + F_{j+\frac{1}{2}} - F_{j-\frac{1}{2}} = A_j \Omega_j \tag{48}$$

in which the integral of the source terms has been approximated by the central-point formula.

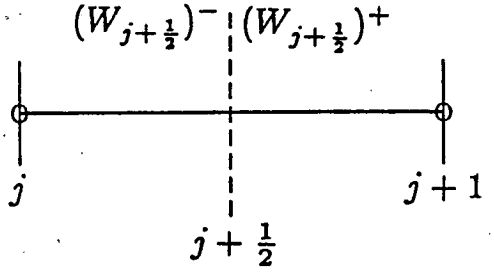

This defines the following explicit conservative scheme

$$W_j^{n+1} = W_j^n - \frac{\Delta t}{A_j}(F_{j+\frac{1}{2}} - F_{j-\frac{1}{2}}) + \Delta t \Omega_j \tag{49}$$

Flux splitting is applied by introducing a flux function $\Phi(u,v)$ consistant with the flux $F(w)$ in the sense that

$$\forall W, \quad \Phi(W,W) = F(W)$$

and letting for all j

$$F_{j+\frac{1}{2}} = \Phi\left((W_{j+\frac{1}{2}})^-; (W_{j+\frac{1}{2}})^+\right)$$

in which $(W_{j+\frac{1}{2}})^-$ is a forward extrapolation of W_j to $x_{j+\frac{1}{2}}$ and $(W_{j+\frac{1}{2}})^+$ is a backward extrapolation of W_{j+1} to $x_{j+\frac{1}{2}}$.
If we choose the Steger-Warming flux [4]

$$\Phi(U,V) = A^+(U)U + A^-(V)V$$

where A^+ and A^- are positive/negative parts of the Jacobian.
In our particular case $F(W) = VW$ then $A(W) = V.Id$, therefore $A^+=A$, $A^-= 0$ and the expression of the flux is simplified

$$\Phi(U,V) = A(U)U = F(U)$$

Consequently

$$F_{j+\frac{1}{2}} = F\left((W_{j+\frac{1}{2}})^-\right)$$

Following van Leer who construct a second-order approximation by letting

$$(W_{j+\frac{1}{2}})^- = W_j + \frac{\Delta x_{j+1}}{2} W_x)_j \tag{50}$$

in which $W_x)_j$ is some gradient of W over the cell C_j. In order to preserve monotonicity the following "limited slope" introduced by van LEER [12] is employed

$$W_x)_j = Moy\left(\frac{W_j - W_{j-1}}{x_j - x_{j-1}}; \frac{W_{j+1} - W_j}{x_{j+1} - x_j}\right)$$

where

$$Moy(a,b) = \frac{(a^2+\varepsilon)b + (b^2+\varepsilon)a}{a^2 + b^2 + \varepsilon} \quad (\varepsilon \text{ very low})$$

In summary, we constructed an explicit scheme which is first order in time and second-order in space.
The initial solution is taken to be uniform, being those immediatly behind the shock (condition at $x = 0$ of the stationary problem). The following residual was evaluated after each time step

$$R = \sqrt{\sum_j A_j \|\Omega_j - \frac{1}{A_j}(F_{j+\frac{1}{2}} - F_{j-\frac{1}{2}})\|^2}$$
$$\sim \|\Omega - \frac{\partial}{\partial x} F(W)\|_{L^2}$$

2.2. *Stability Limit*

A very simplified model of a convection equation with a source term is given by

$$u_t + Cu_x - \lambda u = 0 \tag{51}$$

in which λ represents a typical eigenvalue of the Jacobian $\Omega'(W)$ ($\lambda < 0$) This equation is used here to study the linear stability of the explicit upwind Euler scheme

$$\frac{u_j^{n+1} - u_j^n}{\Delta t} + C\frac{u_j^n - u_{j-1}^n}{\Delta x} - \lambda u_j^n = 0 \tag{52}$$

We study the L^2-stability by Fourier analysis [7]. We put

$$\begin{cases} u_j^{n+1} = ge^{ij\theta} \\ u_j^n = e^{ij\theta} \end{cases}$$

and get

$$\frac{ge^{ij\theta} - e^{ij\theta}}{\Delta t} + C\frac{e^{ij\theta} - e^{i(j-1)\theta}}{\Delta x} - \lambda e^{ij\theta} = 0$$

$$\begin{aligned} g =& 1 - \frac{C\Delta t}{\Delta x}\left(1 - e^{-i\theta}\right) + \lambda\Delta t \\ =& 1 - \frac{C\Delta t}{\Delta x}(1 - \cos\theta) + \lambda\Delta t - i\frac{C\Delta t}{\Delta x}sin\theta \end{aligned}$$

and

$$\begin{aligned} |g|^2 =& 1 + \frac{C^2\Delta t^2}{\Delta x^2}(1 - \cos\theta)^2 + \lambda^2\Delta t^2 - 2\frac{C\Delta t}{\Delta x}(1 - \cos\theta) + 2\lambda\Delta t \\ & - 2\frac{\lambda C\Delta t^2}{\Delta x}(1 - \cos\theta) + \frac{C^2\Delta t^2}{\Delta x^2}sin^2\theta \end{aligned}$$

$$\begin{aligned} |g|^2 \leq 1 \Longleftrightarrow \forall\theta\ ,\ & 2\frac{C^2\Delta t^2}{\Delta x^2}(1 - \cos\theta) + \lambda^2\Delta t^2 - 2\frac{C\Delta t}{\Delta x}(1 - \cos\theta) + 2\lambda\Delta t \\ & - 2\frac{\lambda C\Delta t^2}{\Delta x}(1 - \cos\theta) \leq 0 \\ \Longleftrightarrow \forall\theta\ ,\ & (1 - \cos\theta)\left(2\frac{C^2\Delta t^2}{\Delta x^2} - 2\frac{C\Delta t}{\Delta x} - 2\frac{\lambda C\Delta t^2}{\Delta x}\right) + \lambda^2\Delta t^2 + 2\lambda\Delta t \leq 0 \end{aligned}$$

since $1 - \cos\theta$ varies over the range [0,2] the condition becomes

$$\begin{aligned} & 4\frac{C^2\Delta t^2}{\Delta x^2} - 4\frac{C\Delta t}{\Delta x} - 4\frac{\lambda C\Delta t^2}{\Delta x} + \lambda^2\Delta t^2 + 2\lambda\Delta t \leq 0 \\ & \Delta t^2\left(4\frac{C^2}{\Delta x^2} - 4\frac{\lambda C}{\Delta x} + \lambda^2\right) + \Delta t\left(2\lambda - 4\frac{C}{\Delta x}\right) \leq 0 \\ & \Delta t\left(2\frac{C}{\Delta x} - \lambda\right)^2 + 2\left(\lambda - 2\frac{C}{\Delta x}\right) \leq 0 \end{aligned}$$

or

$$\frac{C\Delta t}{\Delta x} \leq \frac{1}{1 - \frac{\lambda \Delta x}{2C}} \tag{53}$$

By inspection of this formula it appears that a necessary condition of stability is that $\lambda \leq \frac{2C}{\Delta x}$. For the application of concern (endothermic reactions), the eigenvalues of Ω' are negative (see Appendix I); hence this condition is satisfied. Moreover, the right hand side of (53) is positive and less than 1. Therefore, the effect of the source term is as expected to reduced the maximum allowable timestep. For example, in an Euler flow at $M_\infty = 25$, a typical convection velocity is (see Table I): $C = V = 7600$ m/s. Using 300 spatial subdivisions over 10 cm, $\Delta x = \frac{0.1}{300}$ m. The eigenvalues are negative, and typically their moduli vary from 10^4 to 10^8 sec$^-$1. Therefore, $\frac{|\lambda|\Delta x}{C}$ may attain the value: $10^8 \times \frac{0.1}{300}/7600 \sim 4.4$, which corresponds to a CFL number close to 0.2.

In conclusion, the evolution equations for the mass fractions can be stably marched in time by an explicit method. The CFL number is obviously less than 1, but not excessively small, and the approach, if not very efficient is viable.

2.3. *Numerical results*

In the numerical tests, a uniform mesh of 300 points is employed.

The first tests have shown instabilities due to the violent impulsive start, which produces in particular, negative temperature predictions. When this occurs, the value is simply discarded and replaced by $T_j^{n+1} = \frac{1}{2}T_j^n$. This "ad hoc fix up" automatically dissappears after a few iterations, and does not affect the steady-state solution.

The iterative convergence is indicated on Figure 8, where the residual is plotted vs iterations. At the start, the maximum allowable timestep was found to be close to 0.2, as anticipated from a result of the previous section. Further in the iteration, it could slightly be increased to 0.4.

We note that the convergence may be divided in three phases. In a "transient phase" over the first 100 iterations after the impulsive start, the residual decreases rapidly below 10^{-3}. Then we observe a phase of stagnation of the residual over some 1500 iterations. Finally, the scheme enters the asymptotic convergence. The stagnation phase is referred to as the "convective phase".Its existence is attribued to the fact that the amplification matrix is defective. This phenomenon is explained in [10] and will be commented further in a separate publication [11].

Intermediate solutions (Figures 9, 10, 11 and 12) illustrate the spatially hyperbolic nature of the problem: when t increases, the information travels in the direction of increasing x.

At the steady state, the solution is identical to that obtained previously by solving the stationary problem.

In conclusion, this explicit method is quite easy to implement but not very efficient since it requires some 1500 iterations to converge. In the next section, the application of an implicit method is examined.

3. Solution of the time-dependant problem by an implicit method

3.1. *Finite-Volume Linearized Euler Implicit Method*

A fully-implicit first-order scheme applied to (46) is given by:

$$\frac{W^{n+1}-W^n}{\Delta t}+F(W^{n+1})_x=\Omega(W^{n+1}) \tag{54}$$

Linearizing $F(W^{n+1})$ and $\Omega(W^{n+1})$ about W^n gives

$$\begin{aligned} F(W^{n+1}) &= F(W^n)+F'(W^n)(W^{n+1}-W^n)+O(\Delta t^2) \\ &= F(W^n)+V(W^{n+1}-W^n)+O(\Delta t^2) \qquad (55) \\ \Omega(W^{n+1}) &= \Omega(W^n)+\Omega'(W^n)(W^{n+1}-W^n)+O(\Delta t^2) \qquad (56) \end{aligned}$$

where we have used the definition $F(W)=VW$, and $F'(W)=V.Id.$ These relations are injected into (54) which is cast into the following delta form:

$$\left(Id-\Delta t\Omega'(W^n)+V\Delta t\frac{\partial}{\partial x}\right)\left(W^{n+1}-W^n\right)=\Delta t\left(\Omega(W^n)-VW_x^n\right) \tag{57}$$

which is the usual linearized Euler implicit method in a time-discrete space-continuous form. A finite-volume formulation of it is obtained by integrating this equation over the cell C_j . To do this, the second-order approximation described in the previous section is employed to evaluate the explicit term, which controls the accuracy of the steady-state solution. However, in the implicit phase which only acts as a preconditioner the simple first-order upwind scheme is applied. This gives the following finite-volume formula:

$$\left((1+\frac{V\Delta t}{A_j})Id-\Delta t\Omega'(W_j^n)\right)\delta W_j-\frac{V\Delta t}{A_j}\delta W_{j-1}=\Delta t\left(\Omega(W_j^n)-\frac{V}{A_j}(W_{j+\frac{1}{2}}-W_{j-\frac{1}{2}})\right)$$

where

$$\delta W = W^{n+1} - W^n = \begin{pmatrix} W_1^{n+1} - W_1^n \\ \vdots \\ W_N^{n+1} - W_N^n \end{pmatrix}$$

Collecting these equations, one gets the following matrix system:

$$A\delta W = B$$

where A is the following block-bidiagonal matrix

$$A = \begin{pmatrix} a_1 & 0 & \dots & 0 \\ b_2 & a_2 & \dots & 0 \\ \vdots & \ddots & \ddots & \vdots \\ 0 & \dots & b_N & a_N \end{pmatrix}$$

in which the 3×3 blocks are defined by:

$$a_i = \left((1 + \frac{V\Delta t}{A_i}) Id - \Delta t \Omega'(W_i^n) \right)$$

$$b_i = -\frac{V\Delta t}{A_i} Id$$

Hence for this one-dimensional spatially hyperbolic problem, the "implicit solution" is trivially performed by one direct sweep.

3.2. *Numerical results*

The computations are carried out in the same conditions as for the explicit scheme, that is, same number of discretization points (300), same initial conditions and same control on the temperature.

The implicit scheme was found to be stable and convergent for very large Courant numbers (up to 3.10^5).

On figure 13, the iterative convergence of the implicit scheme is demonstrated for a Courant number of 10, 100 and 500 respectively, and compared to the convergence of the sequence 2^{-n}. It appears that for large Courant numbers, the implicit scheme in delta form when a second-order half-upwind spatial approximation is employed in combination with a first-order implicit preconditioner, converges iteratively like 2^{-n} independly of the number of spatial subdivisions. In particular, it does not exhibit the "convective phase" during which the residual stagnates at the previous explicit scheme does. We refer to [10] for more details on this point.

On figures 14 and 15, the steady-state solutions are shown for the case of $M_\infty = 25.$. Evidently, the results are identical to those obtained by application of the previous schemes.

IV. CONCLUSIONS

In this report, we considered a model of chemical dissociation and relaxation applicable to the simulation of the hypersonic reactive flow around a space vehicle, such as the European space shuttle HERMES, when reentering athmosphere. A simplified one-dimensional problem was studied, in which the aerodynamic flow properties were fixed to the values they assume behind a strong shock of a hypersonic flowfield.

The calculations were performed successively by three numerical methods: a space-marching technique, and two time-integration schemes (explicit and implicit). This allowed us to identify the principal length and time scales of the reactional scheme and to appreciate the stiffness of the problem.

The linearized Euler implicit method written in delta form with a second-order half-upwind scheme in the explicit phase combined with a first-order upwind implicit preconditioner, was found to be the most efficient time-integration method, since it is stable for Courant numbers up to 3 10^5, and converges (to steady-state) like 2^{-n} independently of the spatial mesh size.

This method is currently extended to the calculation of 2-D Euler flows subject to nonequilibrium real gas effects [7].

V. REFERENCES

[1] J. D. ANDERSON Jr., Modern Compressible Flow With Historical Perspective, Mac Graw Hill Book Co., 1982.

[2] B. STOUFFLET, O. LE BER, Introduction des Equations de la Dissociation Chimique dans un Algorithme de Résolution des Equations d'Euler. Application à un transporteur spatial, private communication.

[3] J. V. RAKICH , H. E. BAILEY , C. PARK, Computation of Nonequilibrium three Dimensional Inviscid Flow over blunt-nosed bodies flying at Supersonic Speeds AIAA Paper No. 75-835-1975.

[4] J. L. STEGER, R. F. WARMING, Flux Vector Splitting of the Inviscid Gasdynamic Equations with application to Finite Difference Methods, J. of Comp. Phys. 40, 263-293, 1981.

[5] Y. P. RAIZER, Y. B. ZEL'DOVICH, Physics of Shock Waves and High-Temperature Hydrodynamics Phenomena, Academic Press, N. Y., 1965.

[6] J-A. DESIDERI, E. HETTENA, Numerical Simulation of Hypersonic Equilibrium-air Reactive Flow, Rapport INRIA No. 716, août 1987.

[7] J-A. DESIDERI, N. GLINSKY, E. HETTENA, First Experiments with an upwind Finite-Volume Solver for 2-D Non-Equilibrium Hypersonic Flow, Rapport INRIA, to appear.

[8] R. COURANT, K. O. FRIEDRICHS, H. LEWY, On the Partial Difference Equations of Mathematical Physics, IBM J. Res. Dev., vol. 11, pp. 215-234, 1967.

[9] F. FEZOUI, Résolution des Equations d'Euler par un schema de van LEER en Eléments Finis, Rapport INRIA No. 358, Janvier 1985.

[10] J-A. DESIDERI, Preliminary Results on the Iterative Convergence of a class of Implicit Schemes, Rapport INRIA No. 490, Février 1986.

[11] J-A. DESIDERI, N. GLINSKY, Diagonalization of a commonly-used Inconsistent Implicit-Scheme, Rapport INRIA, to appear.

[12] B. van LEER, Computational Methods for Ideal Compressible Flow, Computational Fluid Dynamics - Lecture series 1983-04, von Karman Institute for Fluid

Dynamics,1983.

[13] R. BRUN, P. COLAS, P. GUBERNATIS, D. ZEITOUN, Etude théorique du non-equilibre physico-chimique à l'aval d'un choc fort, Contrat d'étude et de recherche AMD-BA, No. 5 - RDMF 86, Rapport Final, Juin 1987.

VI. APPENDIX I: Eigenvalues of the Jacobian matrix Ω'

In the Fourier analysis of Section 2.2, the parameter λ models a typical eigenvalue of the Jacobian matrix Ω'. Hence to illustrate this analysis, and to appreciate the relevant scales for the problem considered, these eigenvalues have been computed numerically as functions of x, and at various times during the convergence process. The results are indicated on Figures 16, 17 and 18 after 1, 10 and 50 iterations respectively ($\Delta t = 0.1298916\ 10^{-3}$).

The eigenvalue λ_1 is found to be real and negative; the range for the modulus is roughly

$$10^6 \leq |\lambda_1| \leq 10^8$$

(the unit is sec^{-1}).

Except in a very narrow region near $x = 0.24$ cm, the other two eigenvalues are also found real and negative, and the approximate ranges are:

$$10^5 \leq |\lambda_2| \leq 10^8$$
$$10^4 \leq |\lambda_3| \leq 10^8$$

In the region of exception, λ_2 and λ_3 are complex conjugate, with a real part close to -10^6 and the imaginary part close to 10^4.

We note that real negative eigenvalues act as dissipation.

STATIONARY CASE

$M_\infty = 25.$

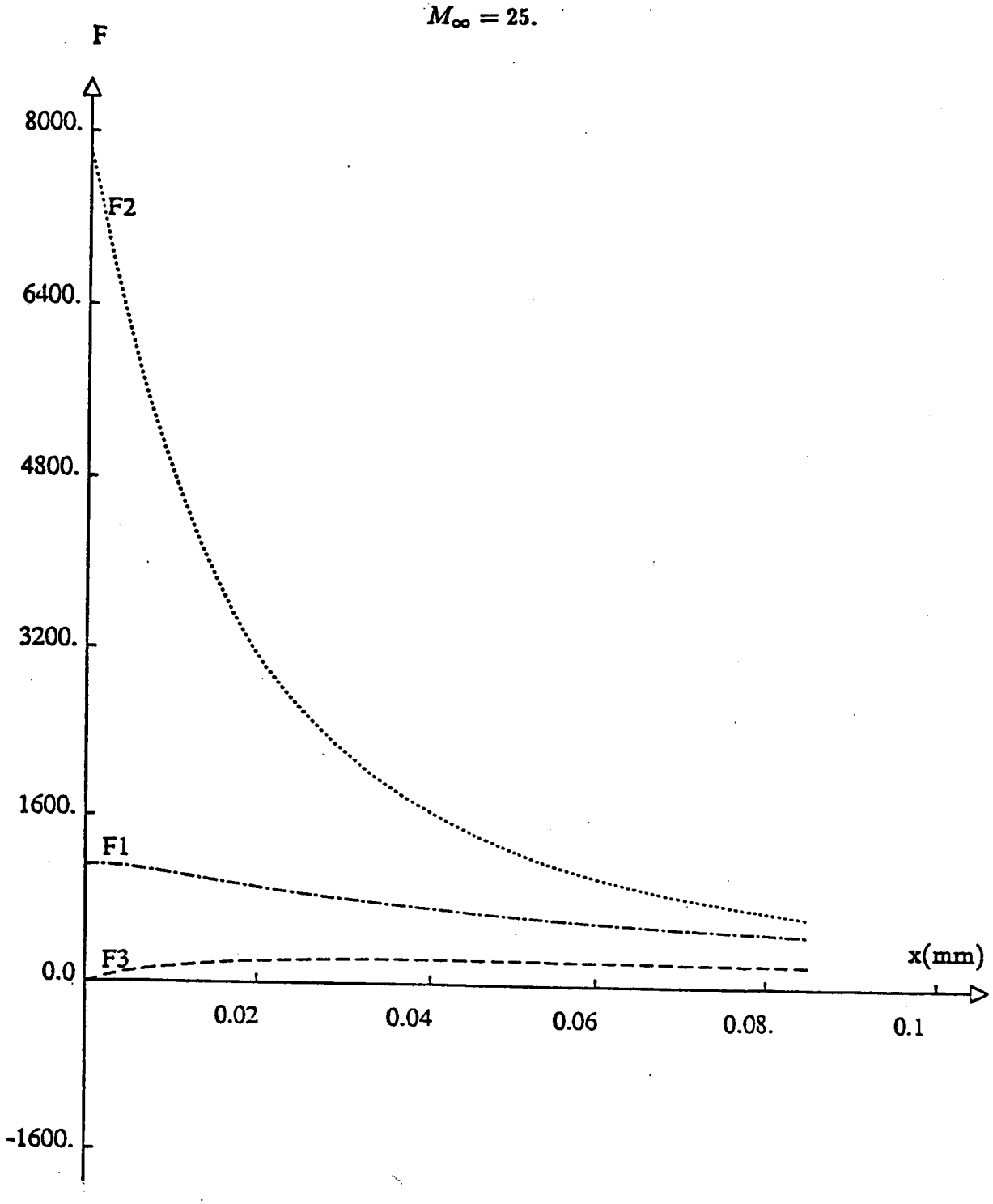

SOURCE TERMS

$$(Y_i)_x = F_i(Y,T)$$

figure 1

STATIONARY CASE

$M_\infty = 20.$

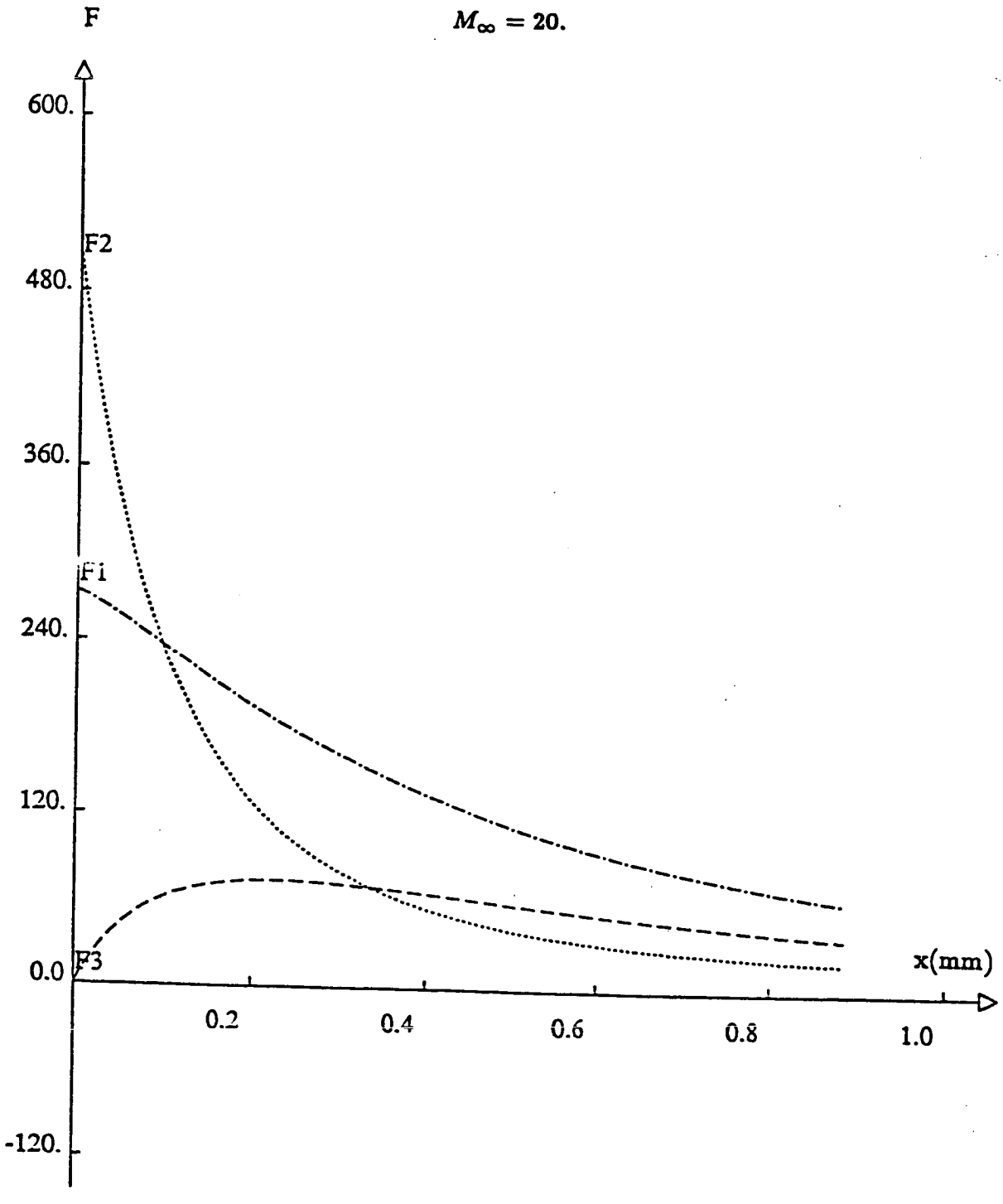

SOURCE TERMS

$$(Y_i)_z = F_i(Y, T)$$

figure 2

STATIONARY CASE

$M_\infty = 15.$

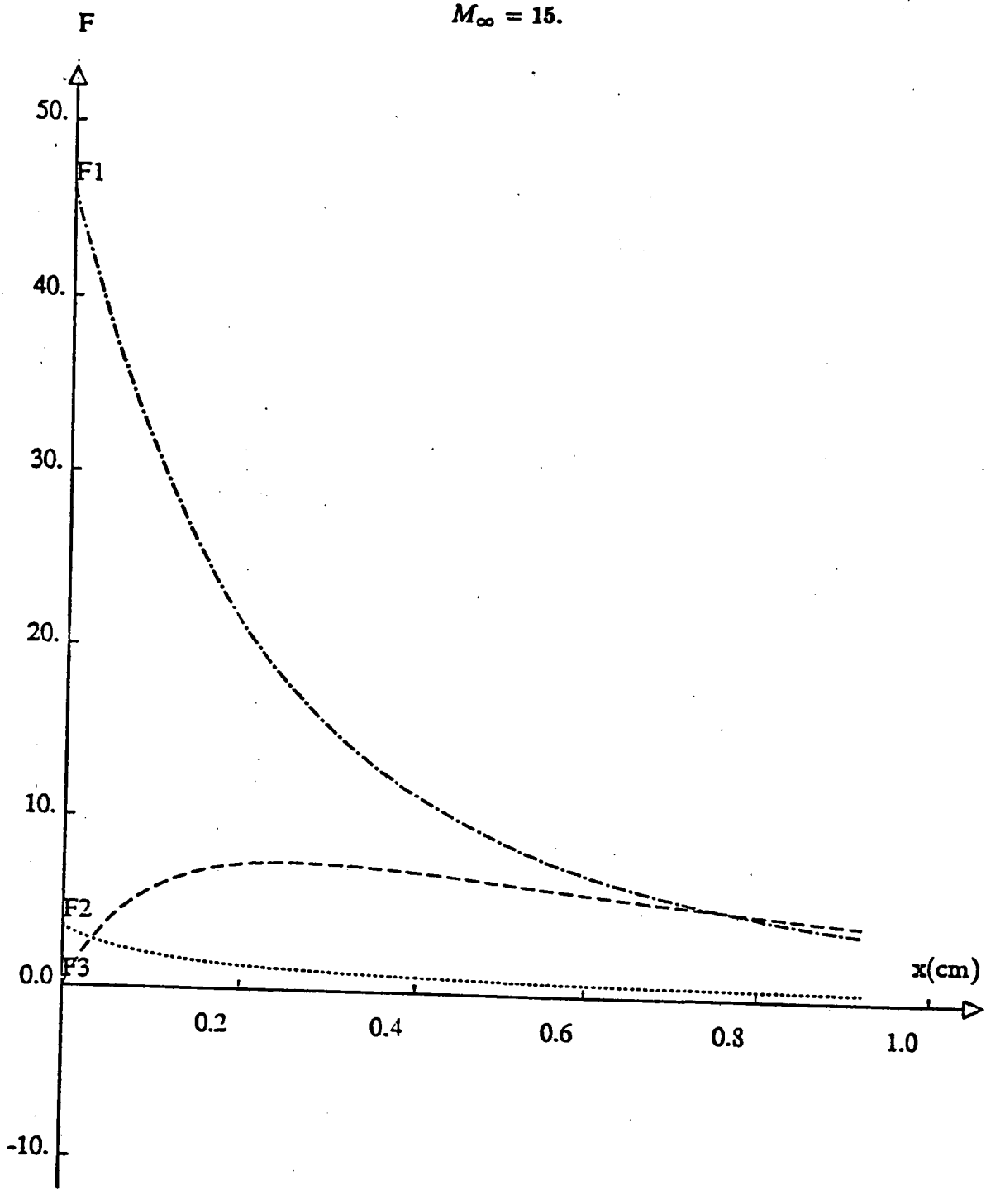

SOURCE TERMS

$$(Y_i)_x = F_i(Y,T)$$

figure 3

Adapted mesh for the space-marching
Runge-Kutta method
($M_\infty = 25, 20, 15$)

figure 4

figure 5

STATIONARY CASE

$M_\infty = 25.$

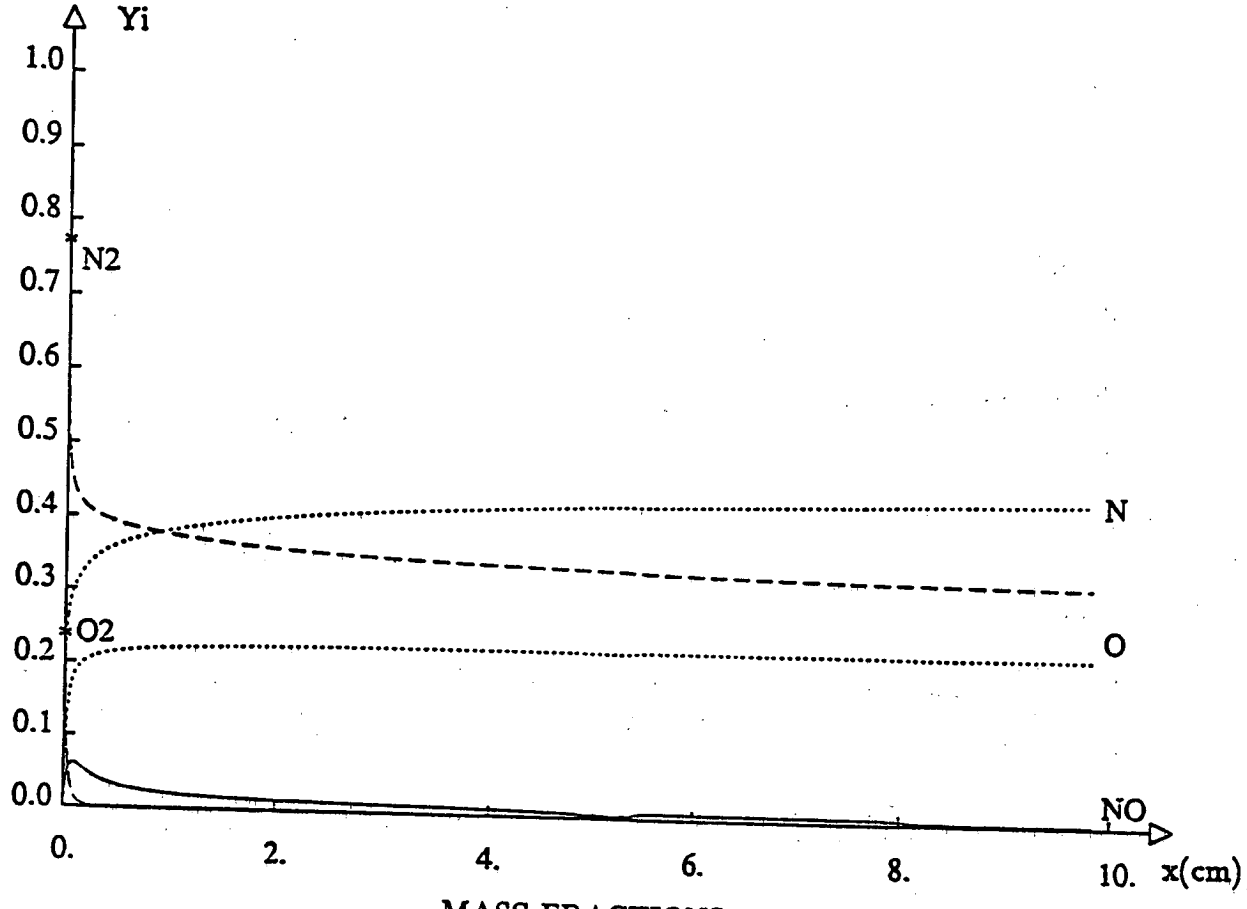

MASS FRACTIONS

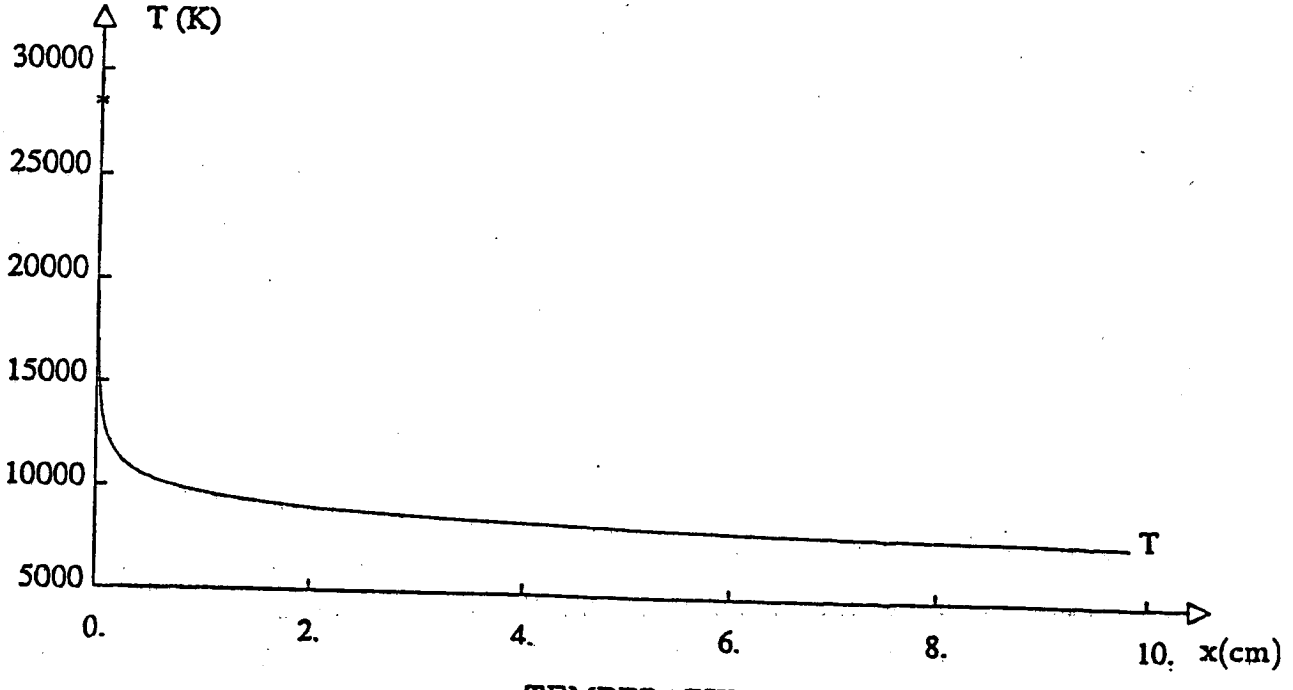

TEMPERATURE

$T_{max} = 28291.K \quad T_{min} = 7919.K$

figure 6

STATIONARY CASE

$M_\infty = 20.$

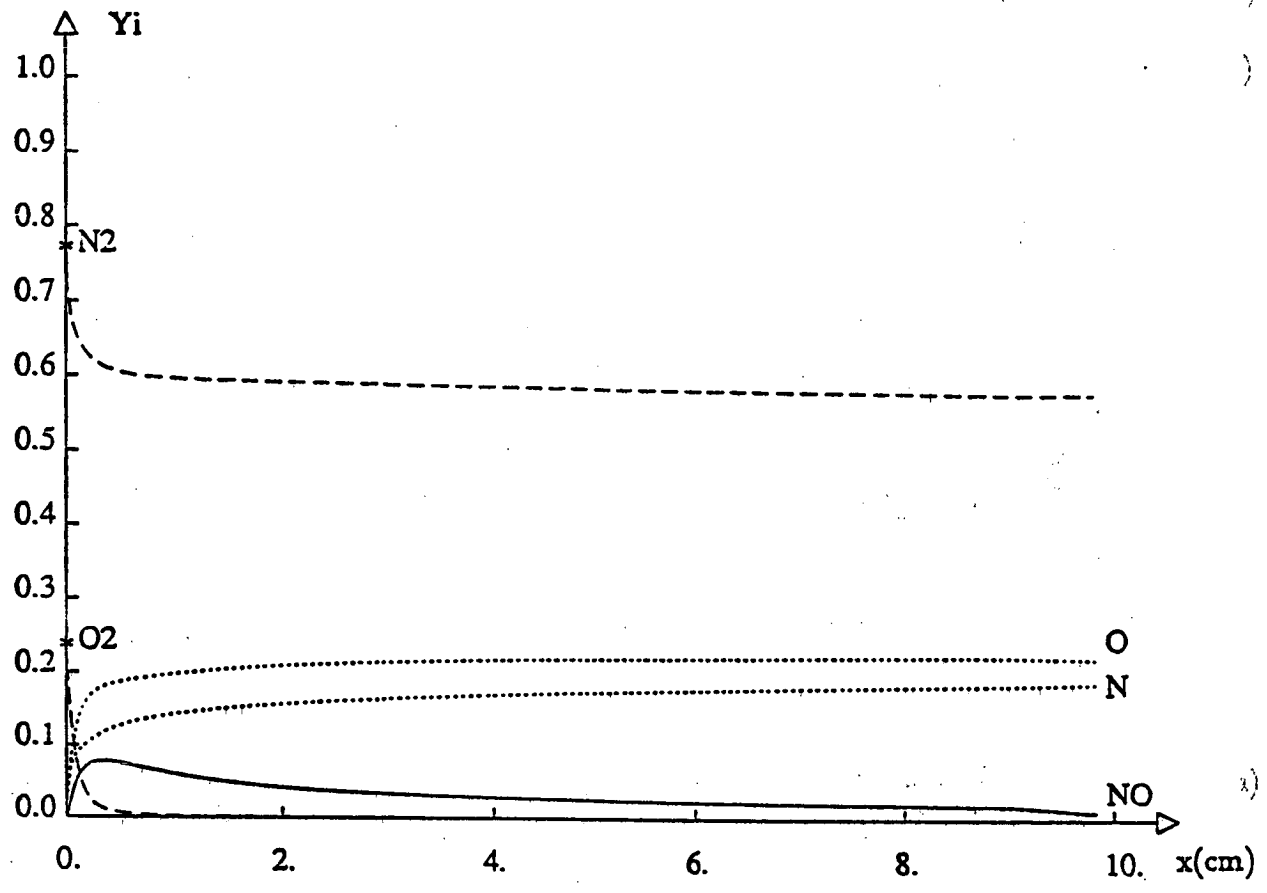

MASS FRACTIONS

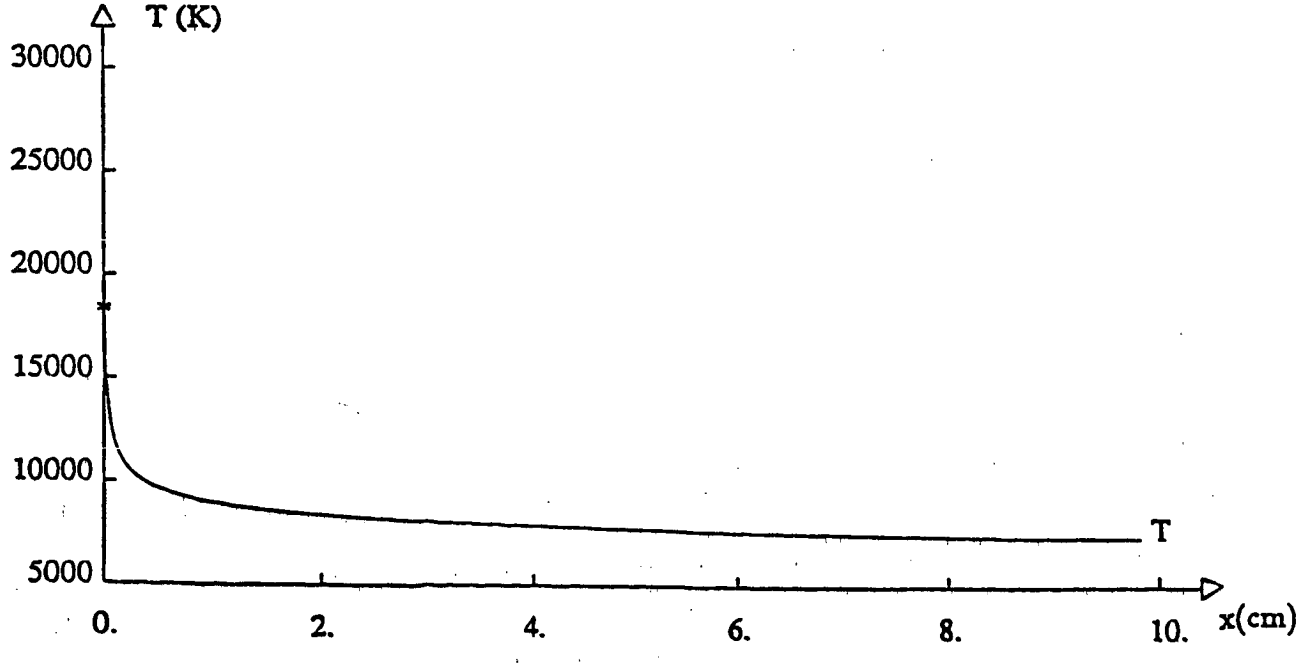

TEMPERATURE

$T_{max} = 18185.K \quad T_{min} = 7349.K$

figure 7

STATIONARY CASE

$M_\infty = 15.$

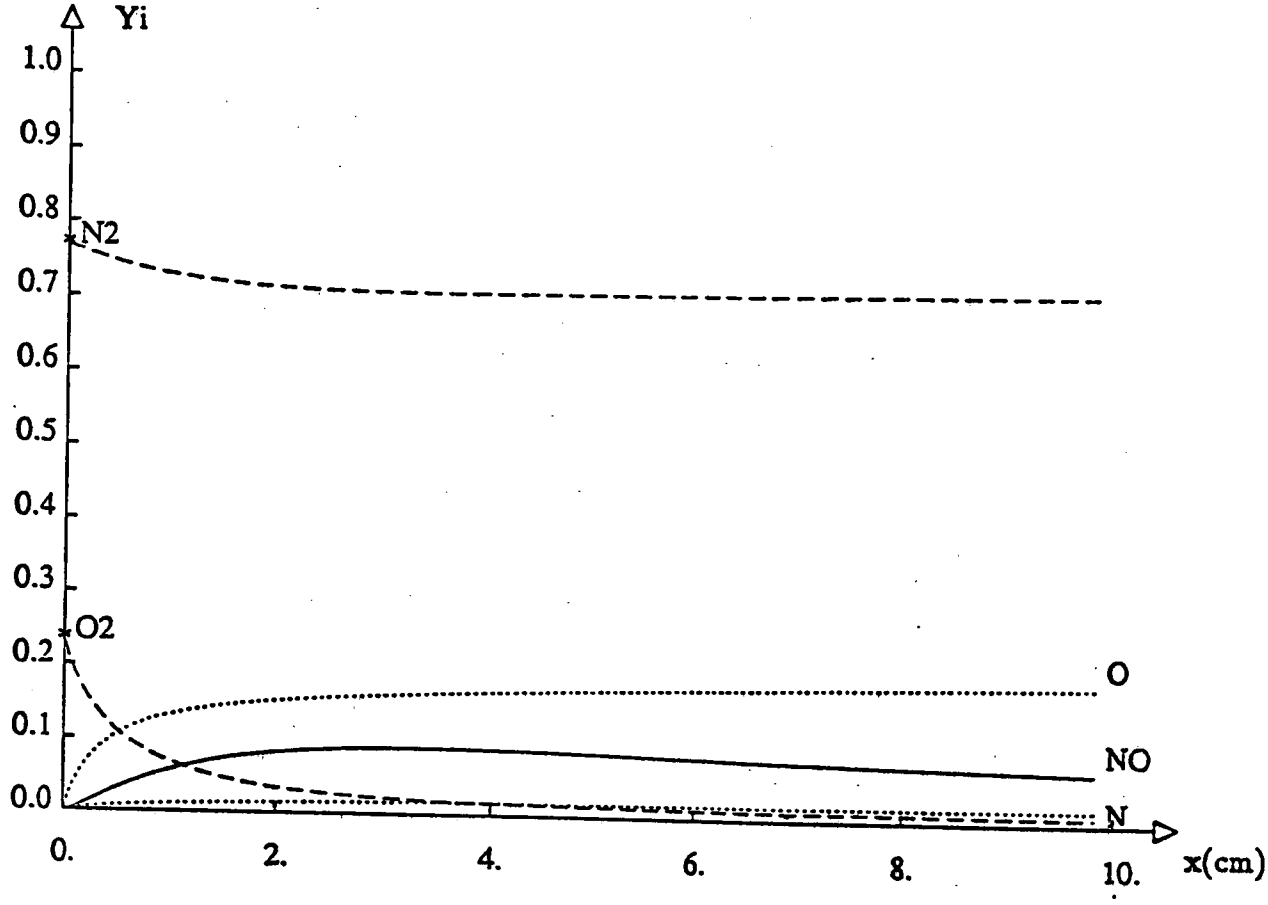

MASS FRACTIONS

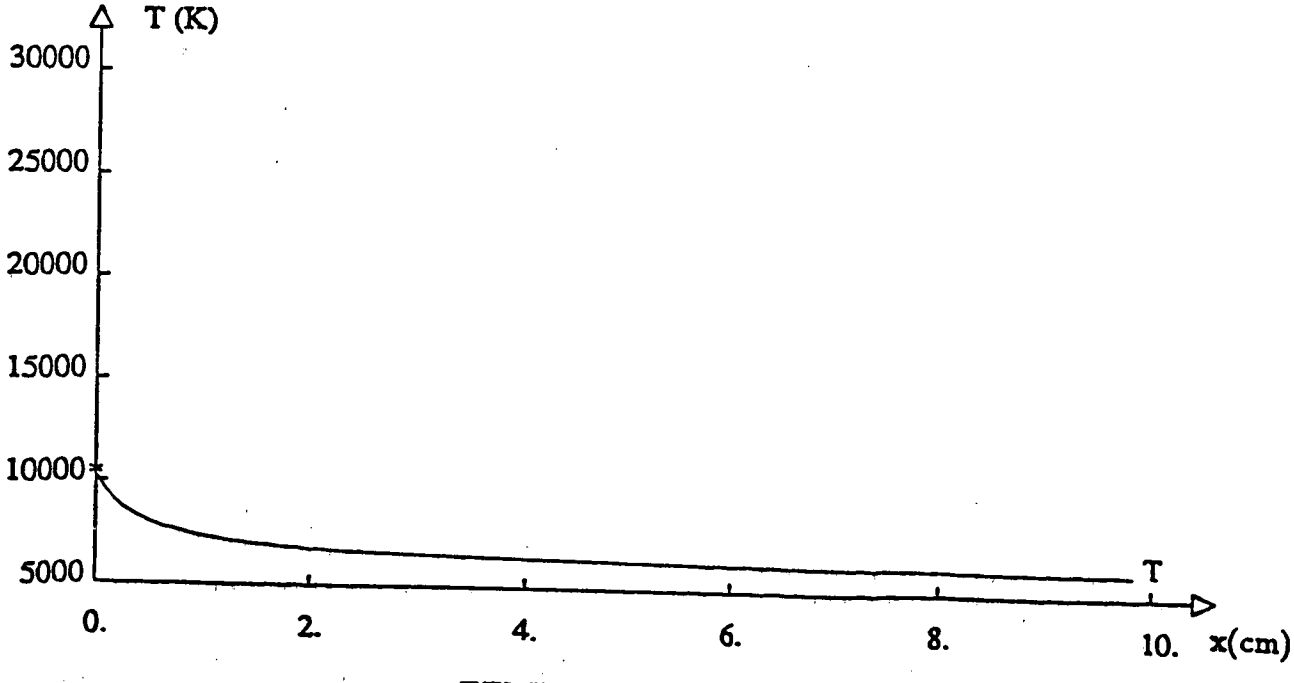

TEMPERATURE

$T_{max} = 10324.K \quad T_{min} = 6137.K$

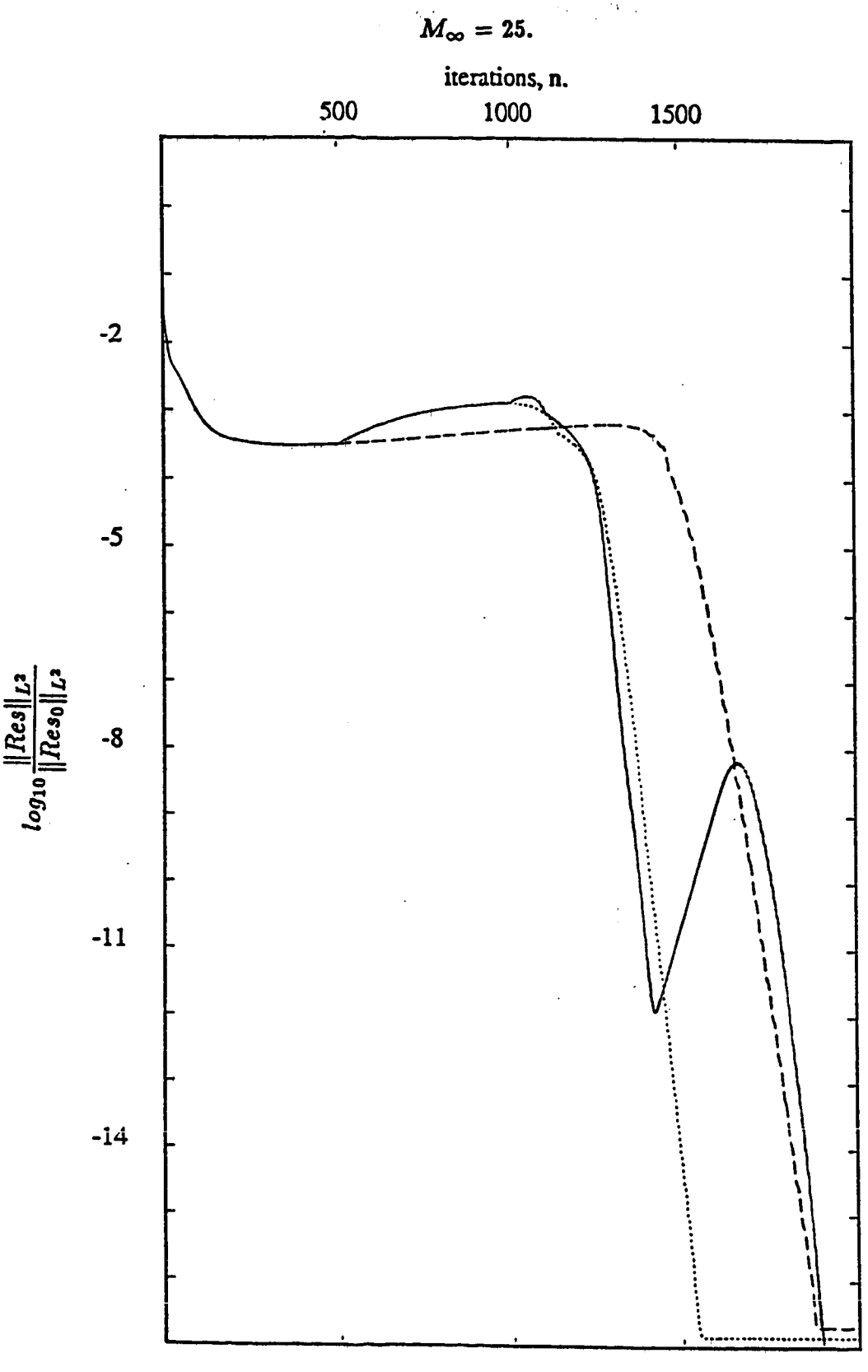
$M_\infty = 25.$
iterations, n.
500
1000
1500
-2
-5
-8
-11
-14
$log_{10} \frac{\|Res\|_{L^2}}{\|Res_0\|_{L^2}}$
CFL=0.2,0.3,0.4(/500 it)
CFL=0.2
CFL=0.2(500 it),0.3

figure 8

figure 9

SECOND-ORDER EXPLICIT SCHEME

$M_\infty = 25.$

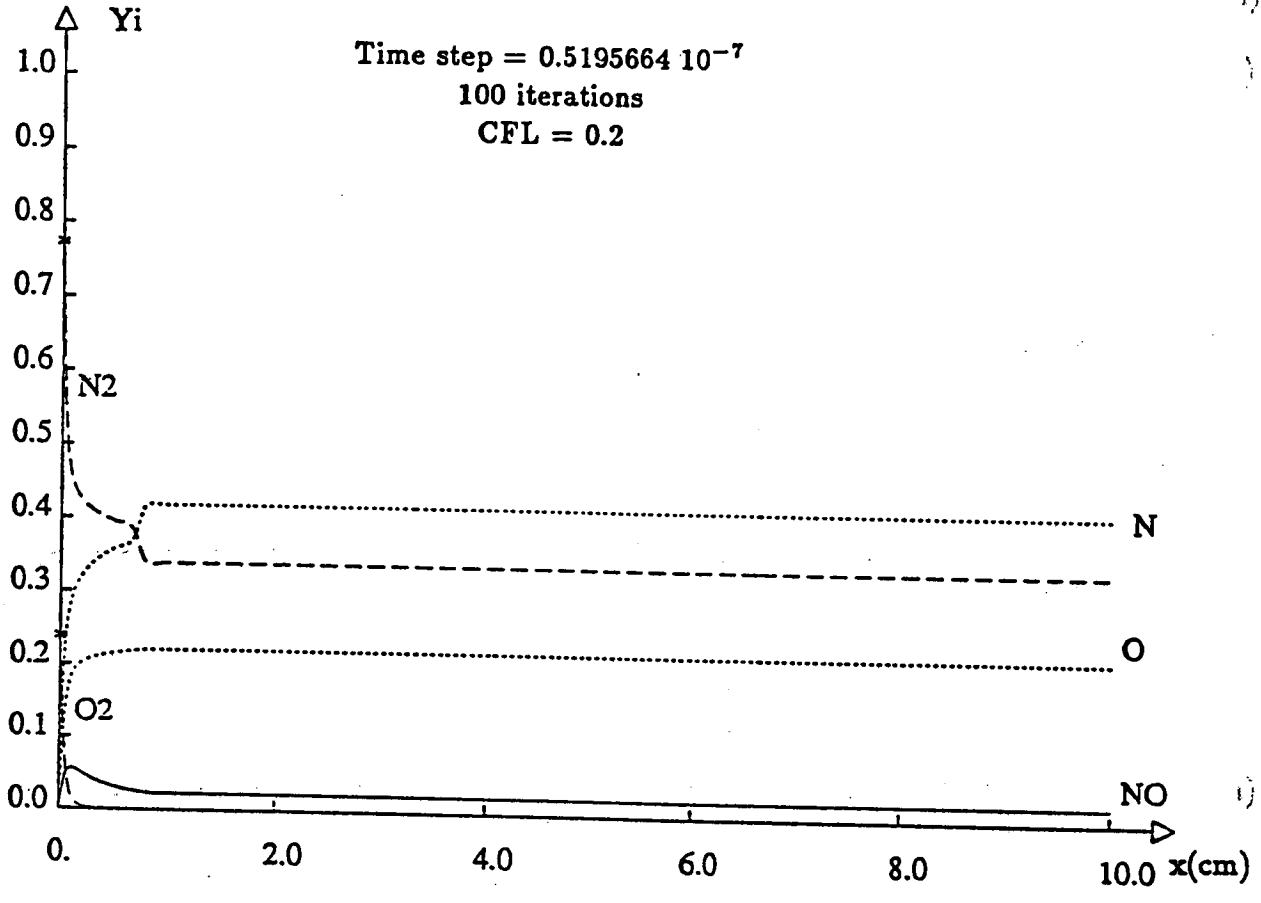

Time step = $0.5195664\ 10^{-7}$
100 iterations
CFL = 0.2

MASS FRACTIONS

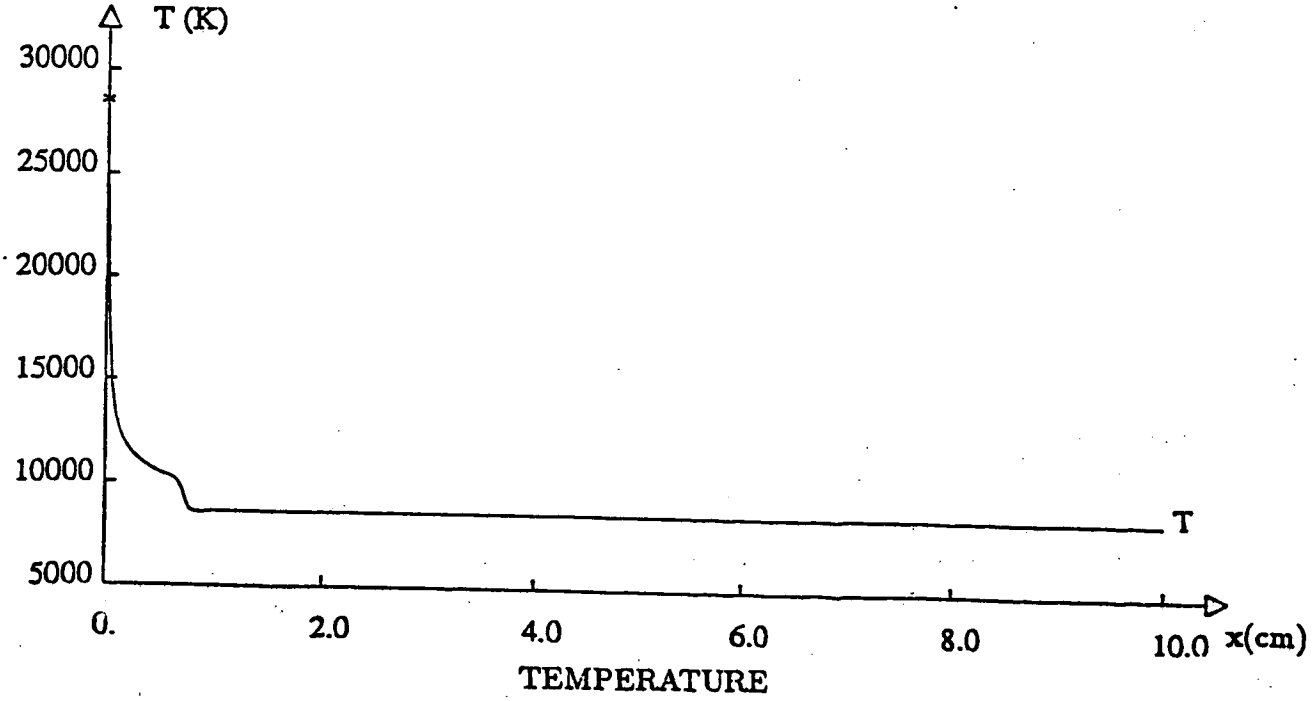

TEMPERATURE

$T_{max} = 28321.K \quad T_{min} = 8629.K$

figure 10

SECOND-ORDER EXPLICIT SCHEME

$M_\infty = 25.$

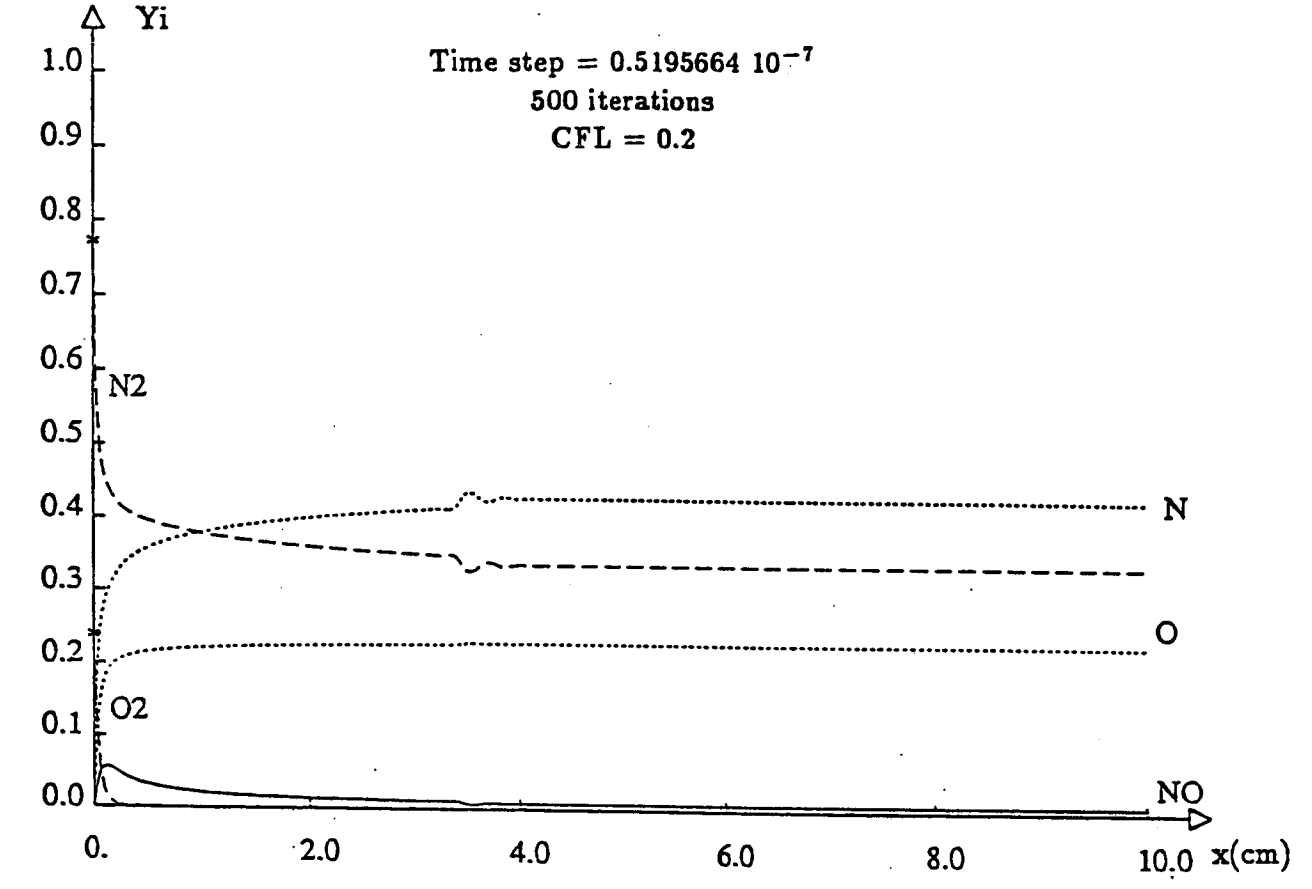

MASS FRACTIONS

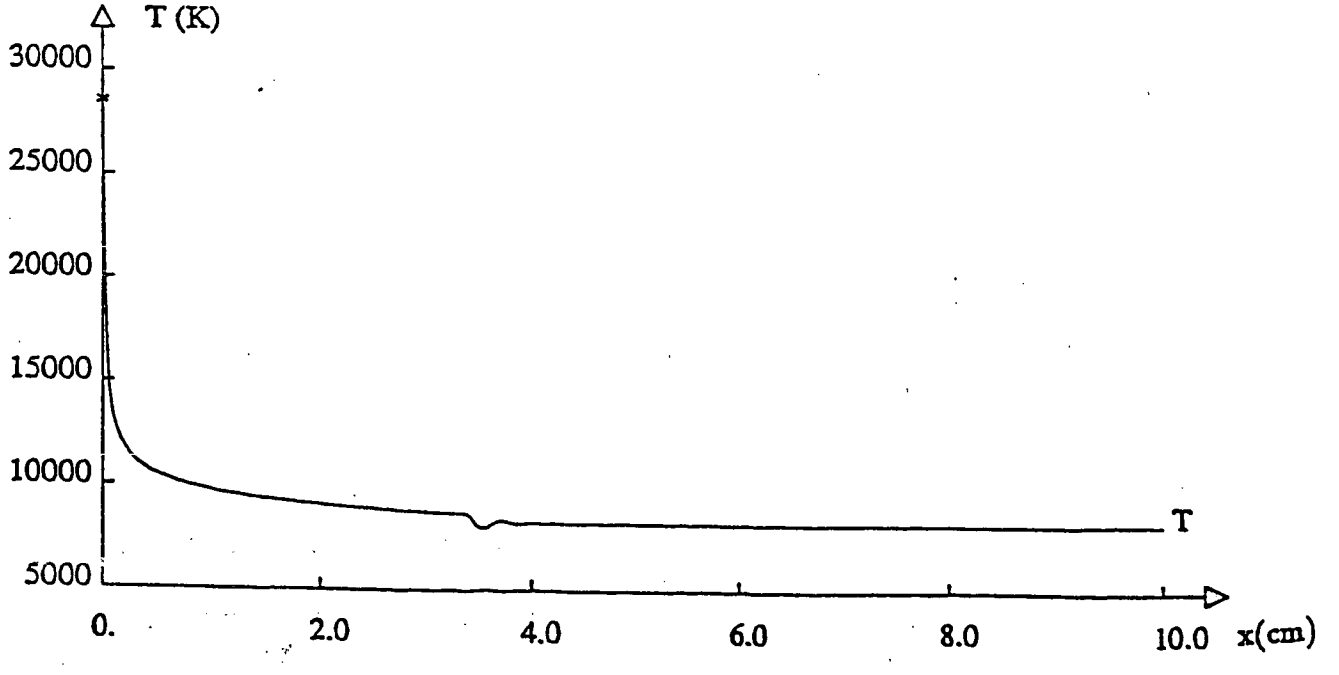

TEMPERATURE

$T_{max} = 28321.K \quad T_{min} = 8268.K$

figure 11

SECOND-ORDER EXPLICIT SCHEME

$M_\infty = 25.$

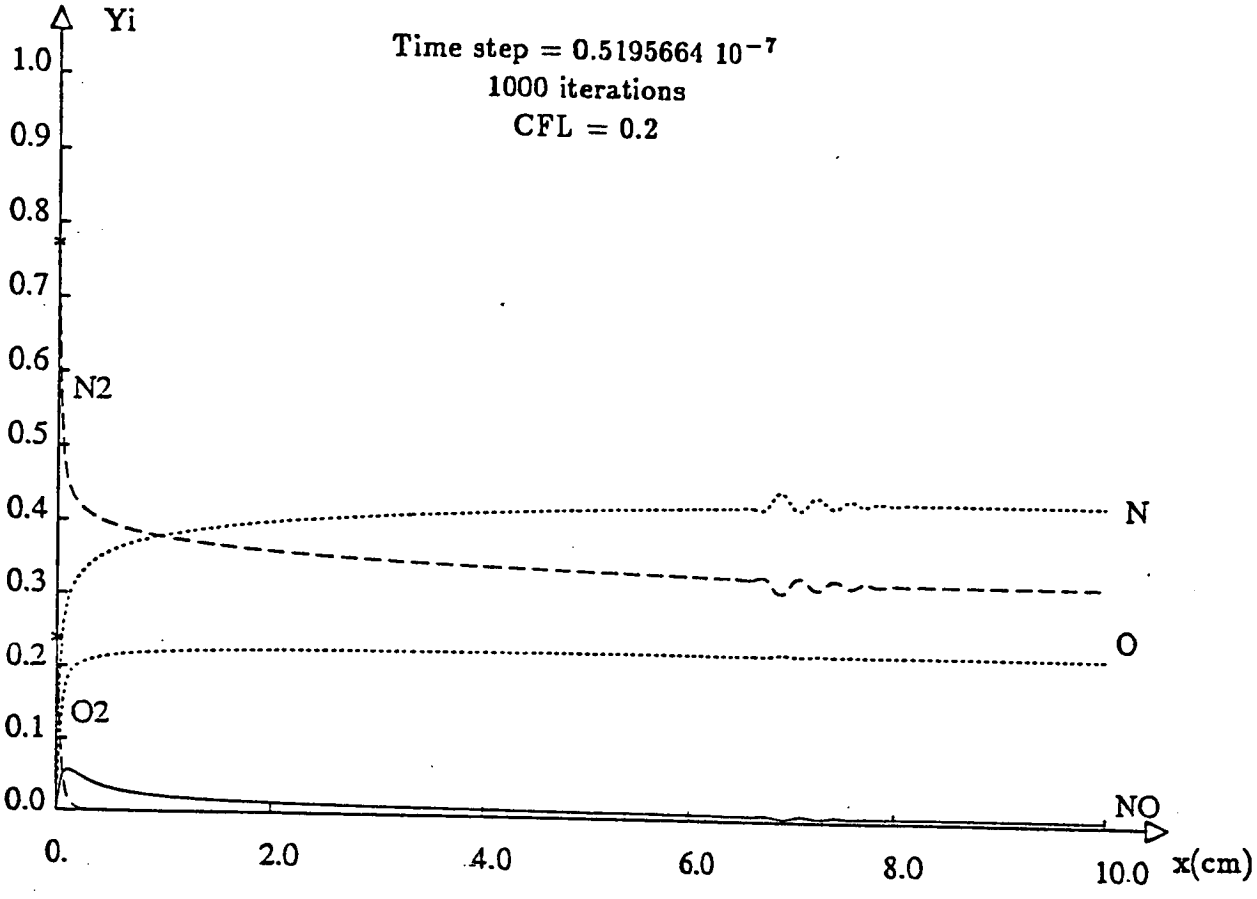

Time step = 0.5195664 10^{-7}
1000 iterations
CFL = 0.2

MASS FRACTIONS

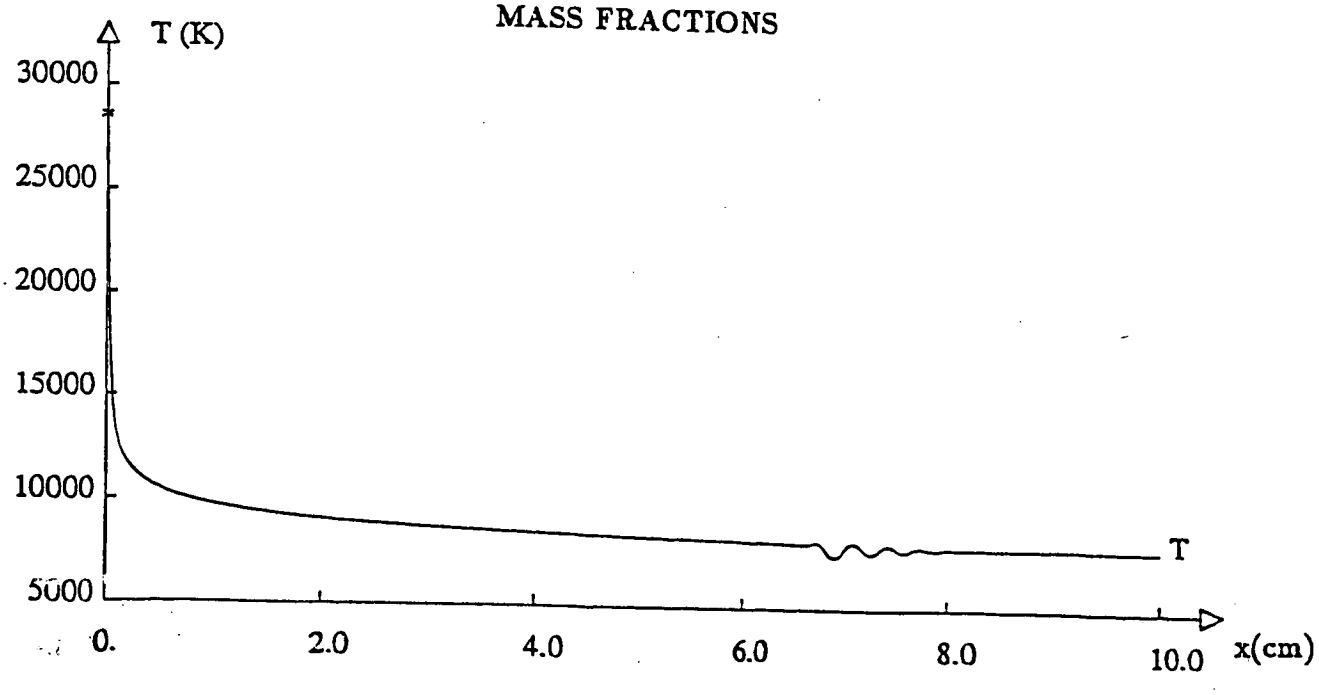

TEMPERATURE

$T_{max} = 28321.K \quad T_{min} = 7972.K$

figure 12

SECOND-ORDER EXPLICIT SCHEME

$M_\infty = 25.$

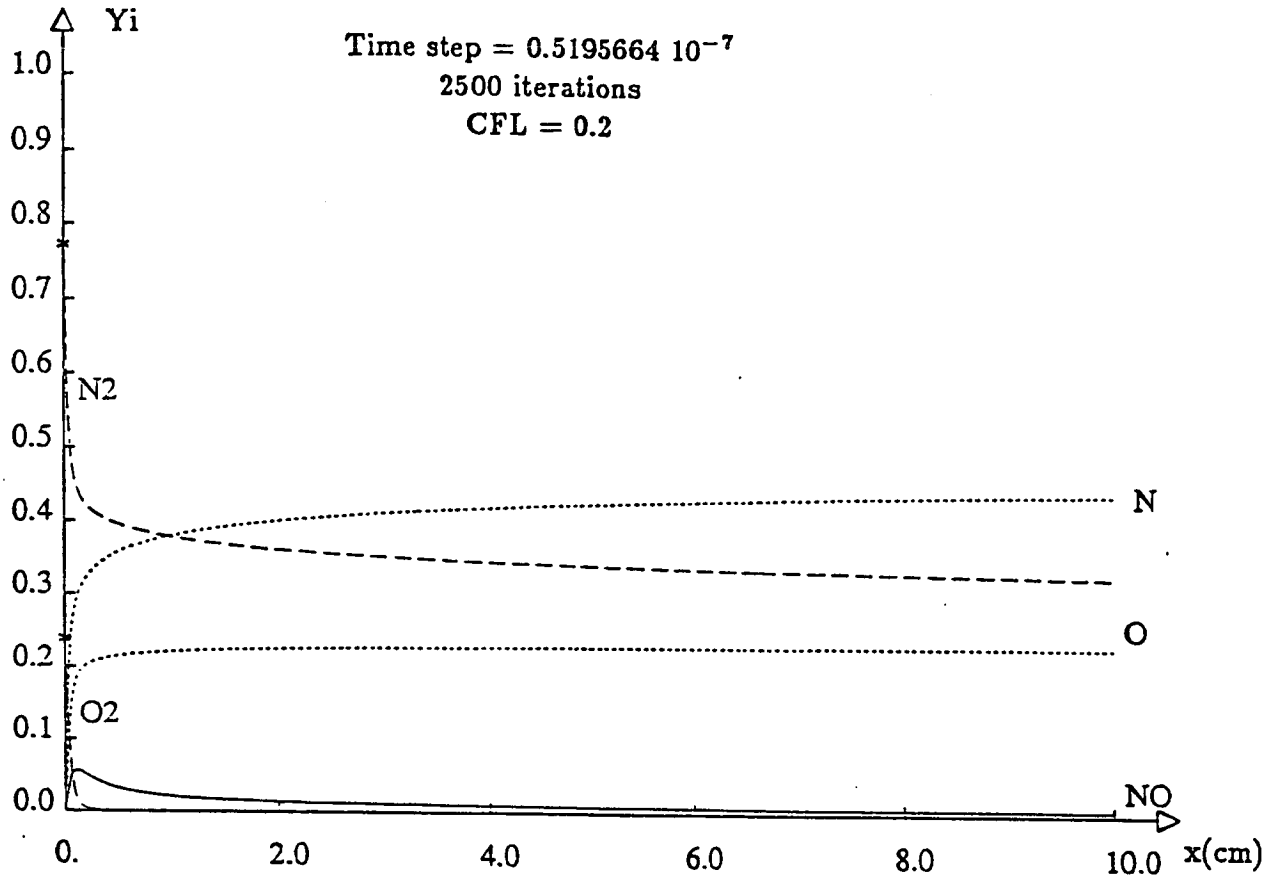

MASS FRACTIONS

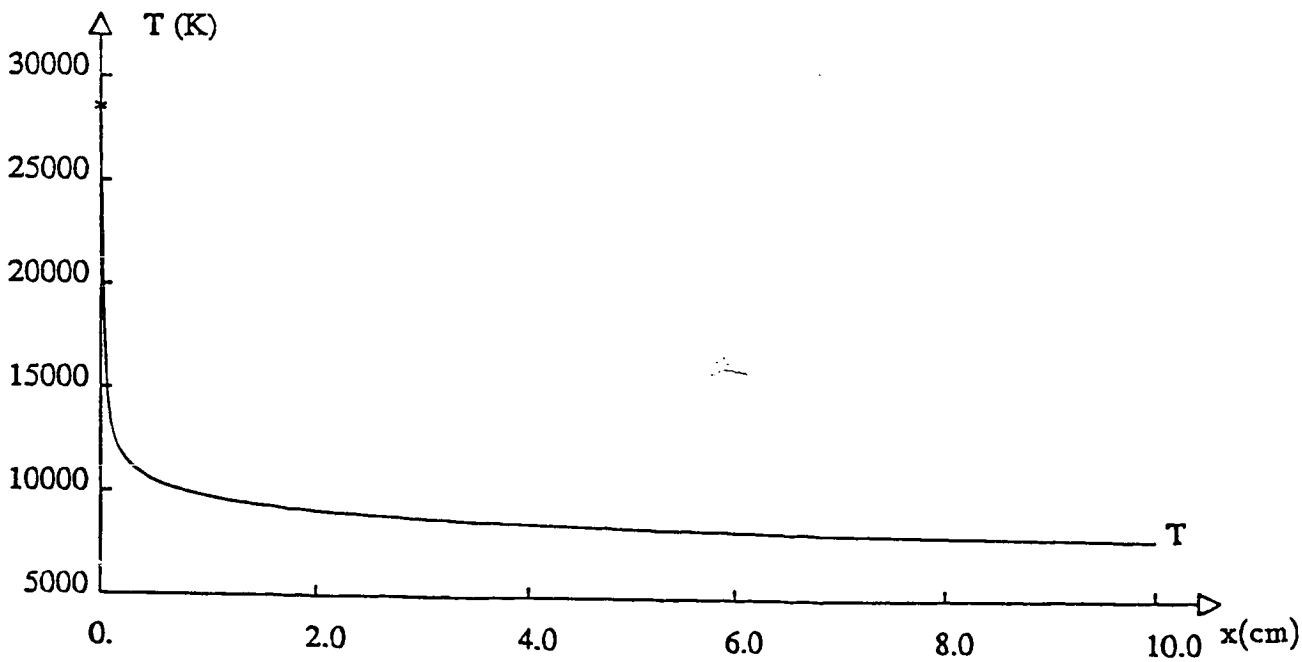

TEMPERATURE

$T_{max} = 28321.K \quad T_{min} = 7925.K$

$M_\infty = 25.$

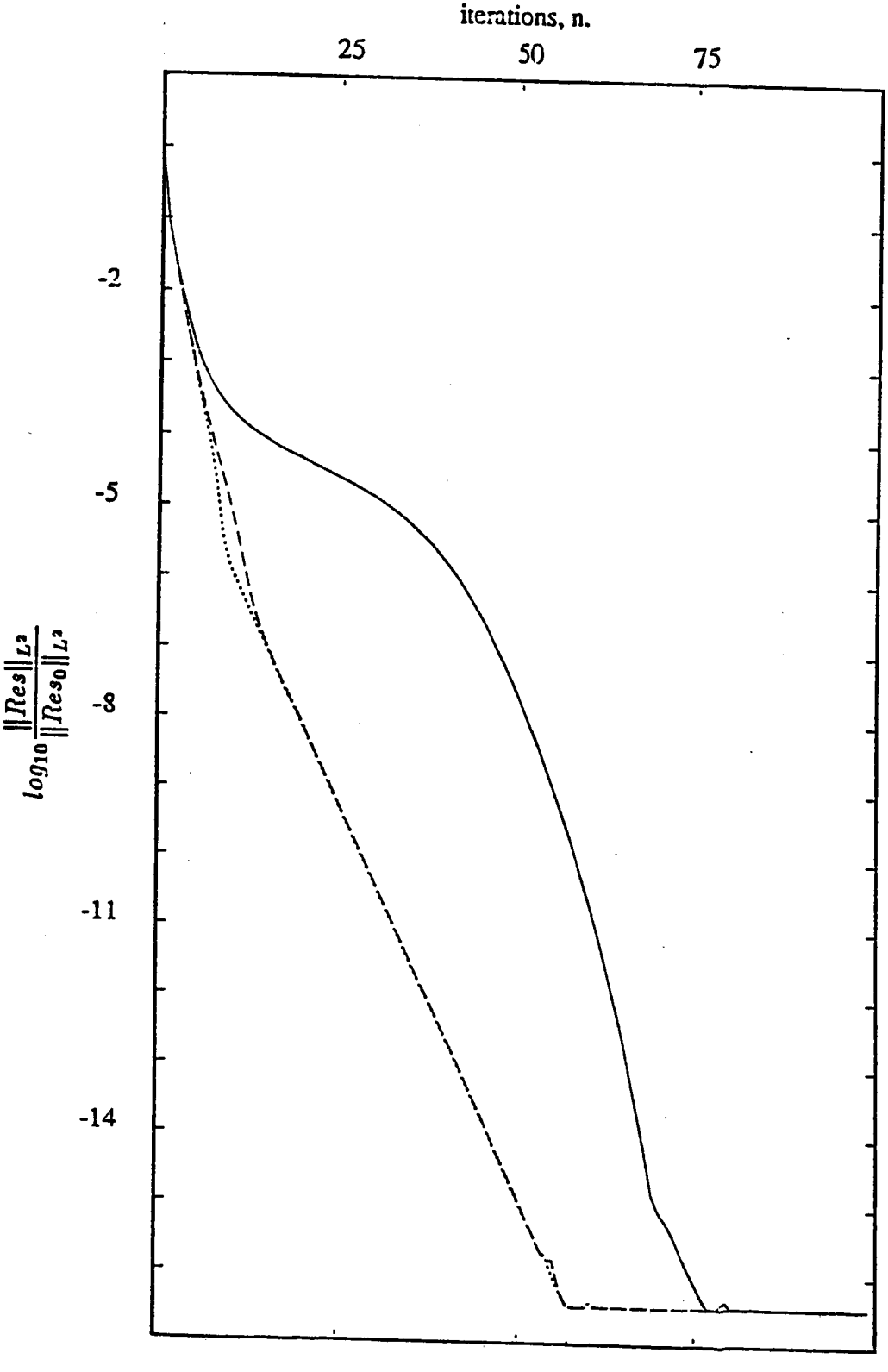

figure 13

figure 14

SECOND-ORDER IMPLICIT SCHEME

$M_\infty = 25.$

Time step = $0.1298916\ 10^{-3}$
58 iterations
CFL = 500.

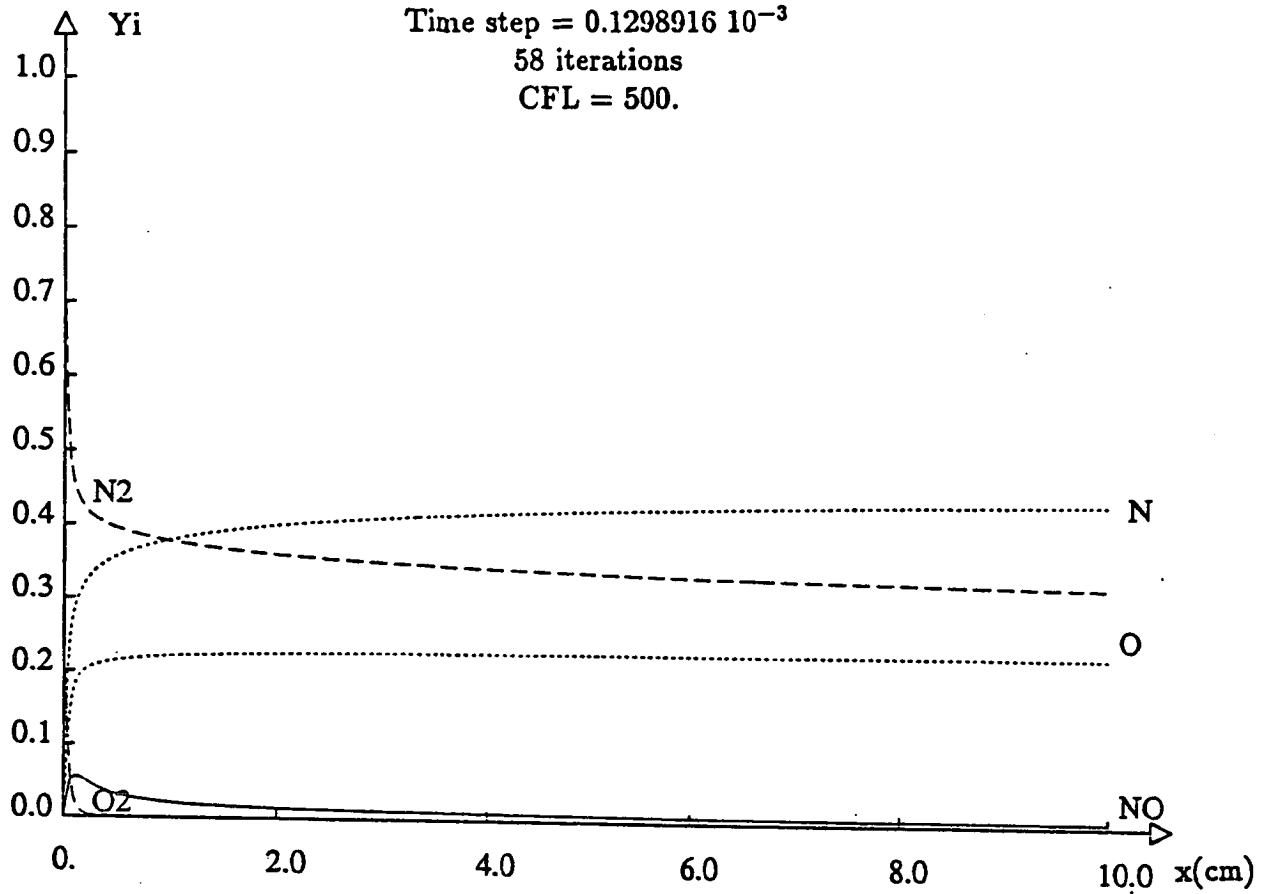

MASS FRACTIONS

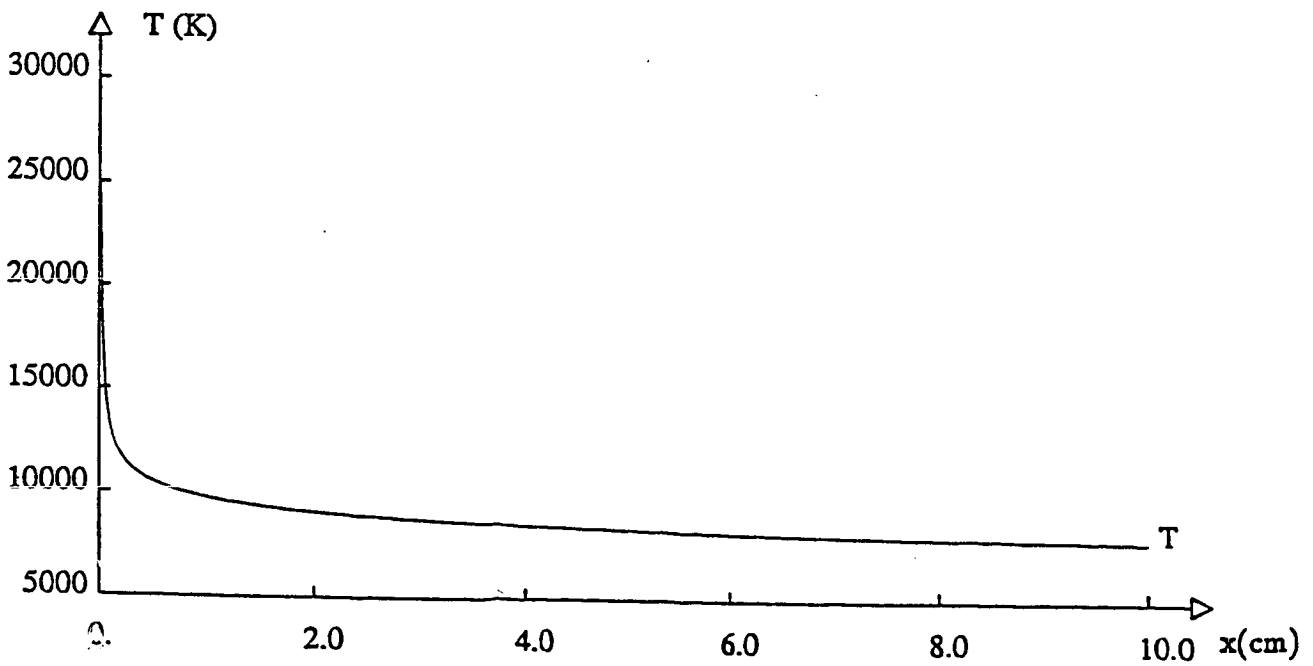

TEMPERATURE

$T_{max} = 28321.K \quad T_{min} = 7925.K$

figure 15

SECOND-ORDER IMPLICIT SCHEME

$M_\infty = 25.$

Time step = $0.7793498\ 10^{-1}$
10 iterations
CFL = 3.10^5

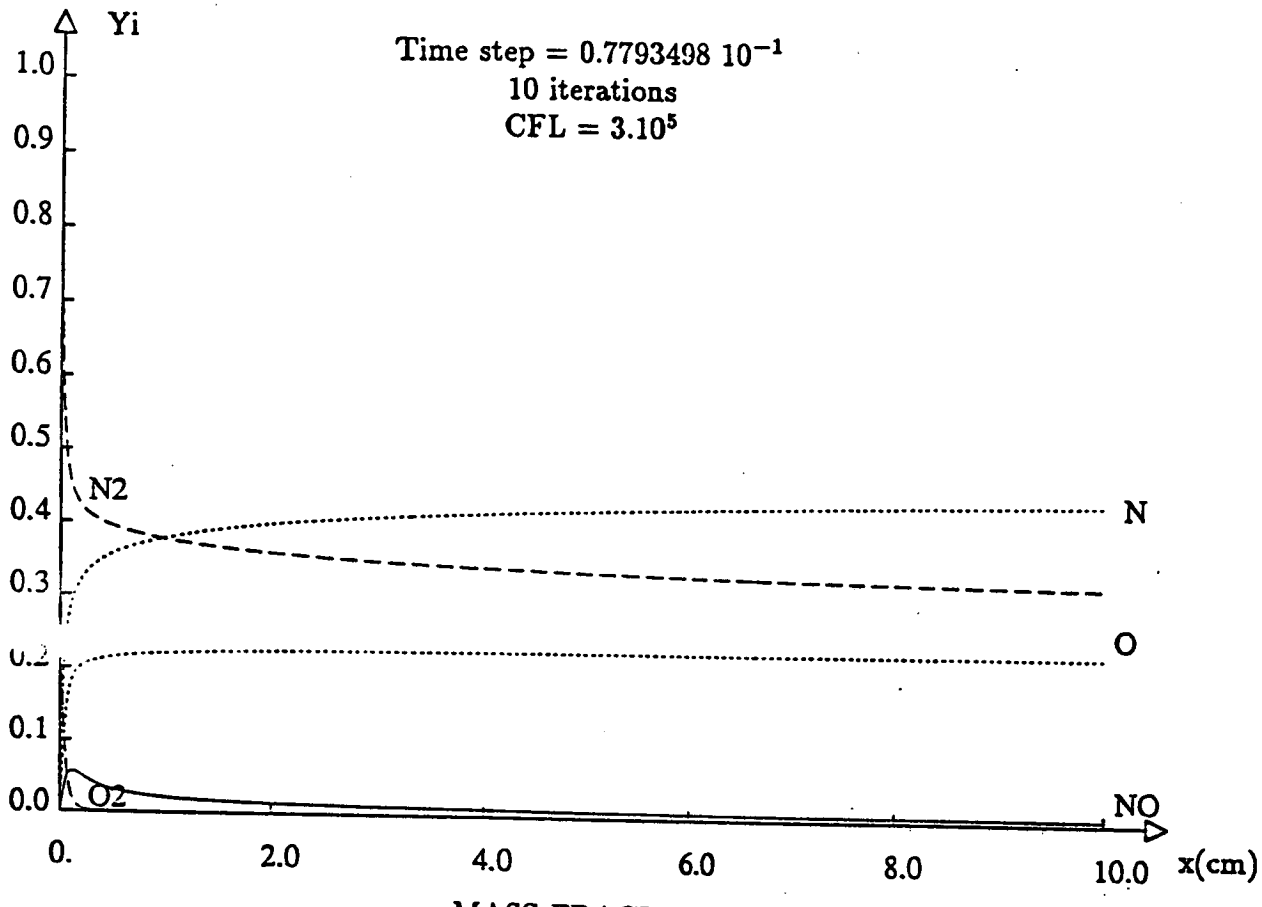

MASS FRACTIONS

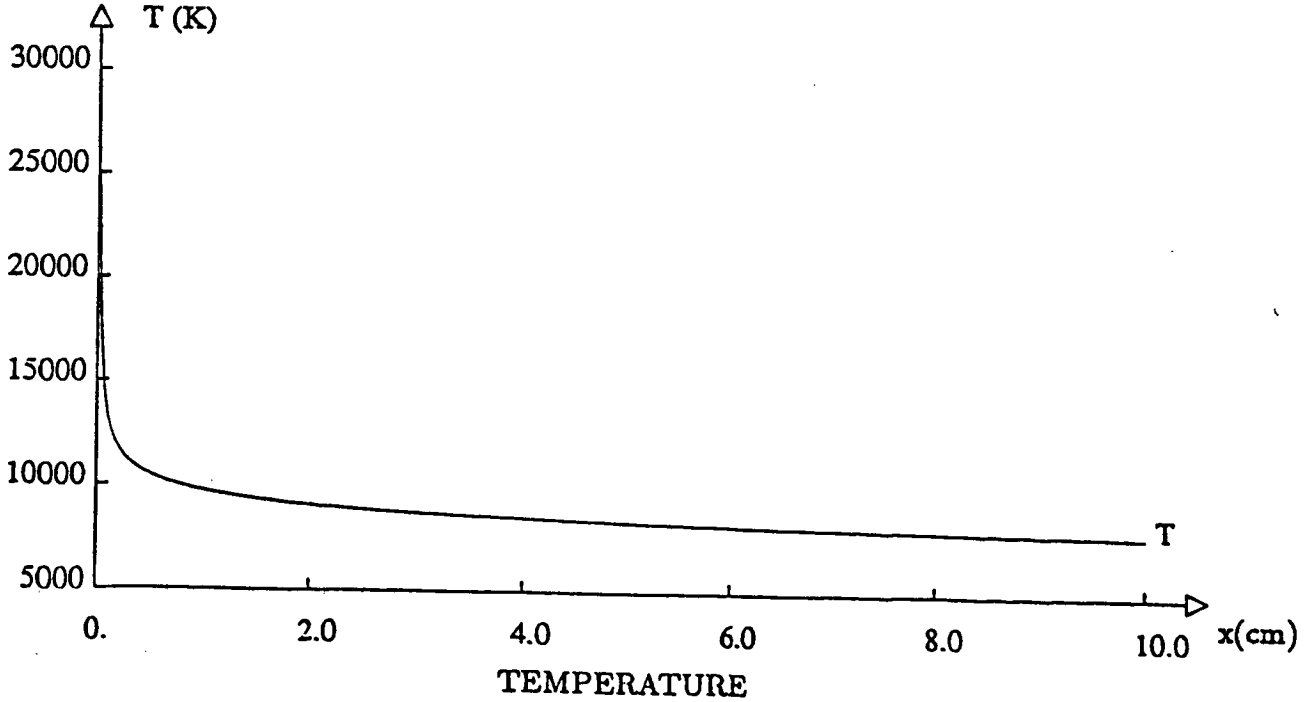

TEMPERATURE

$T_{max} = 28321.K \quad T_{min} = 7925.K$

EIGENVALUES OF Ω'

$M_\infty = 25.$

1 iteration
CFL = 500.

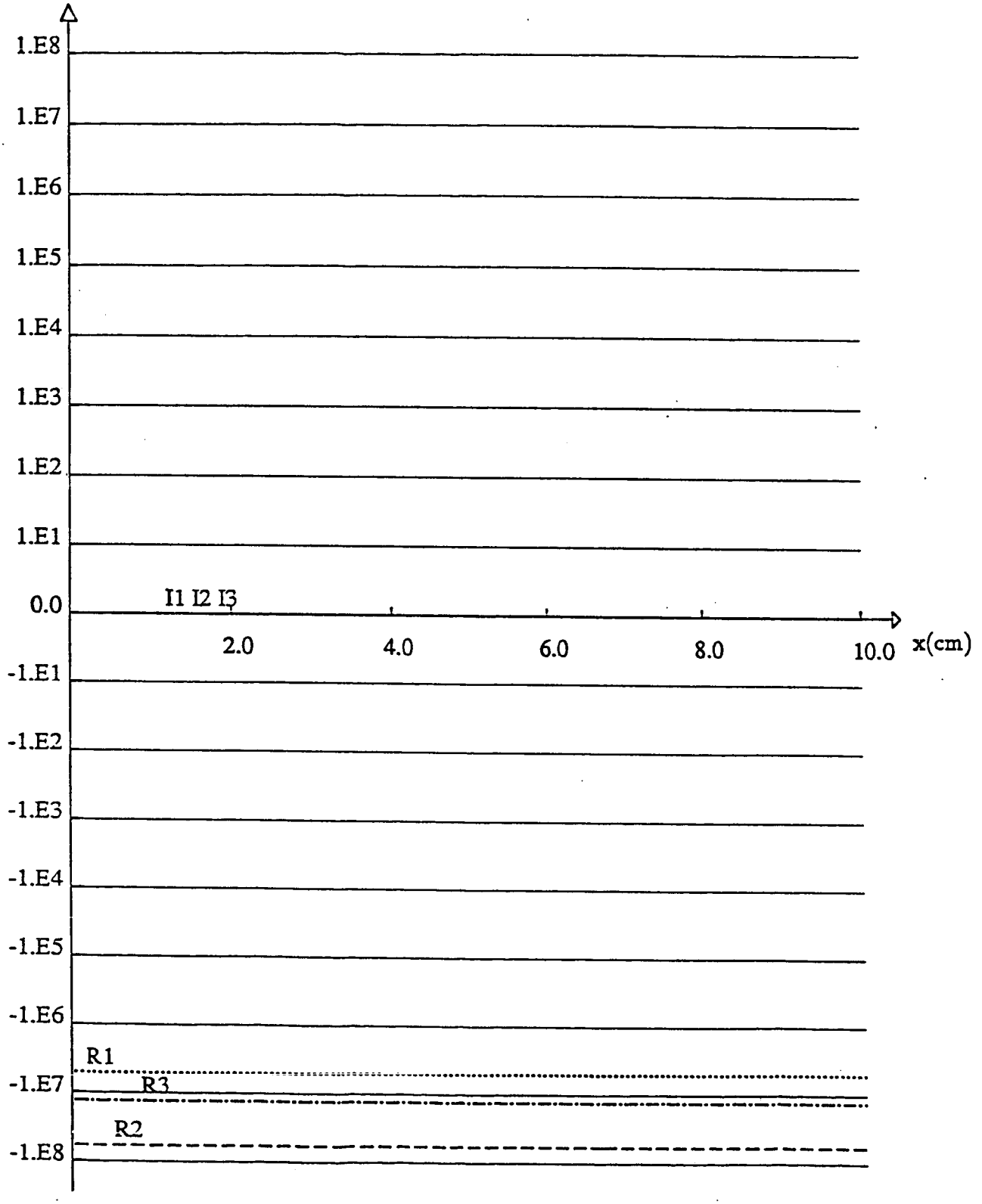

figure 16

EIGENVALUES OF Ω'

$M_\infty = 25.$

5 iterations
CFL = 500.

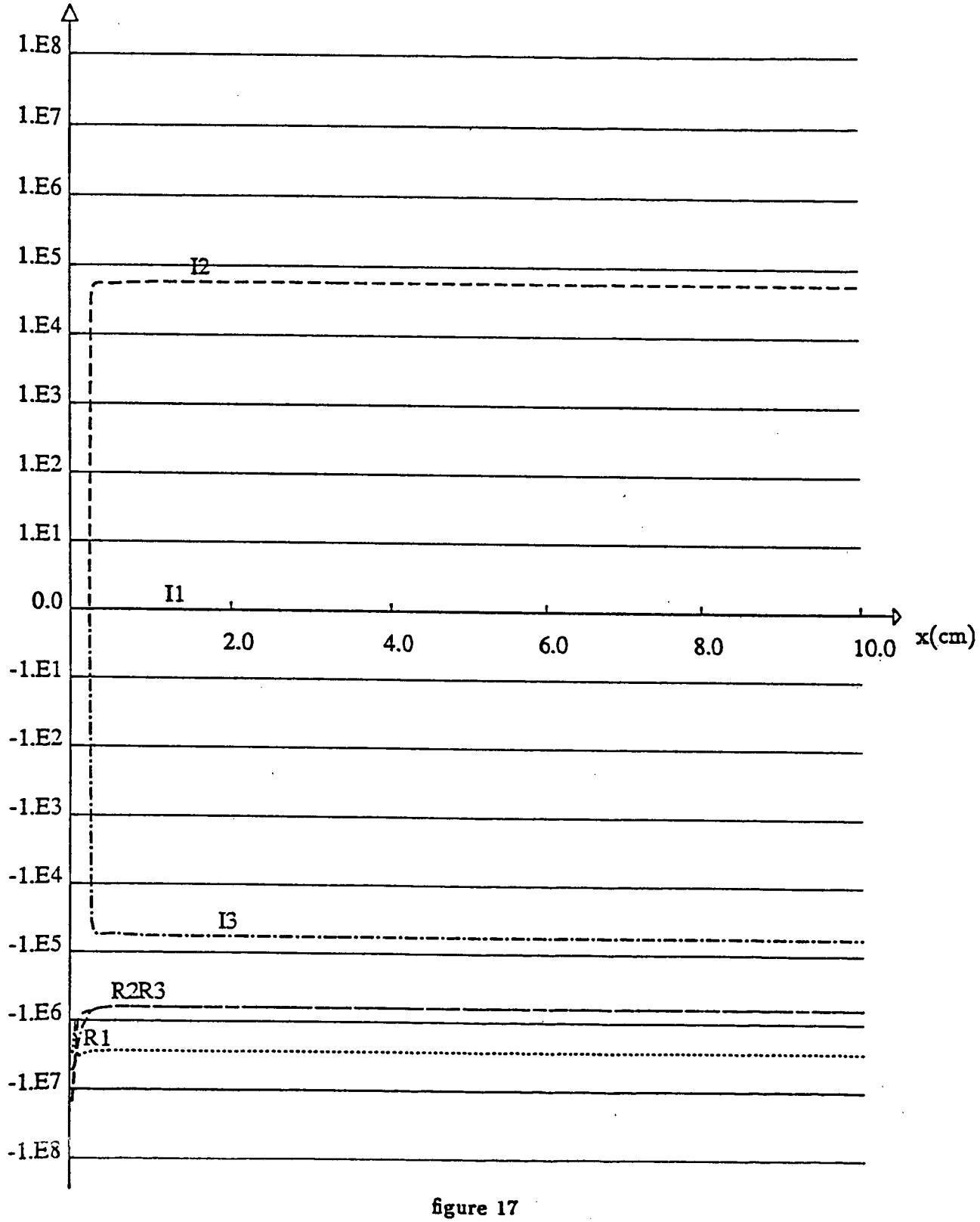

figure 17

EIGENVALUES OF Ω'

$M_\infty = 25.$

50 iterations
CFL = 500.

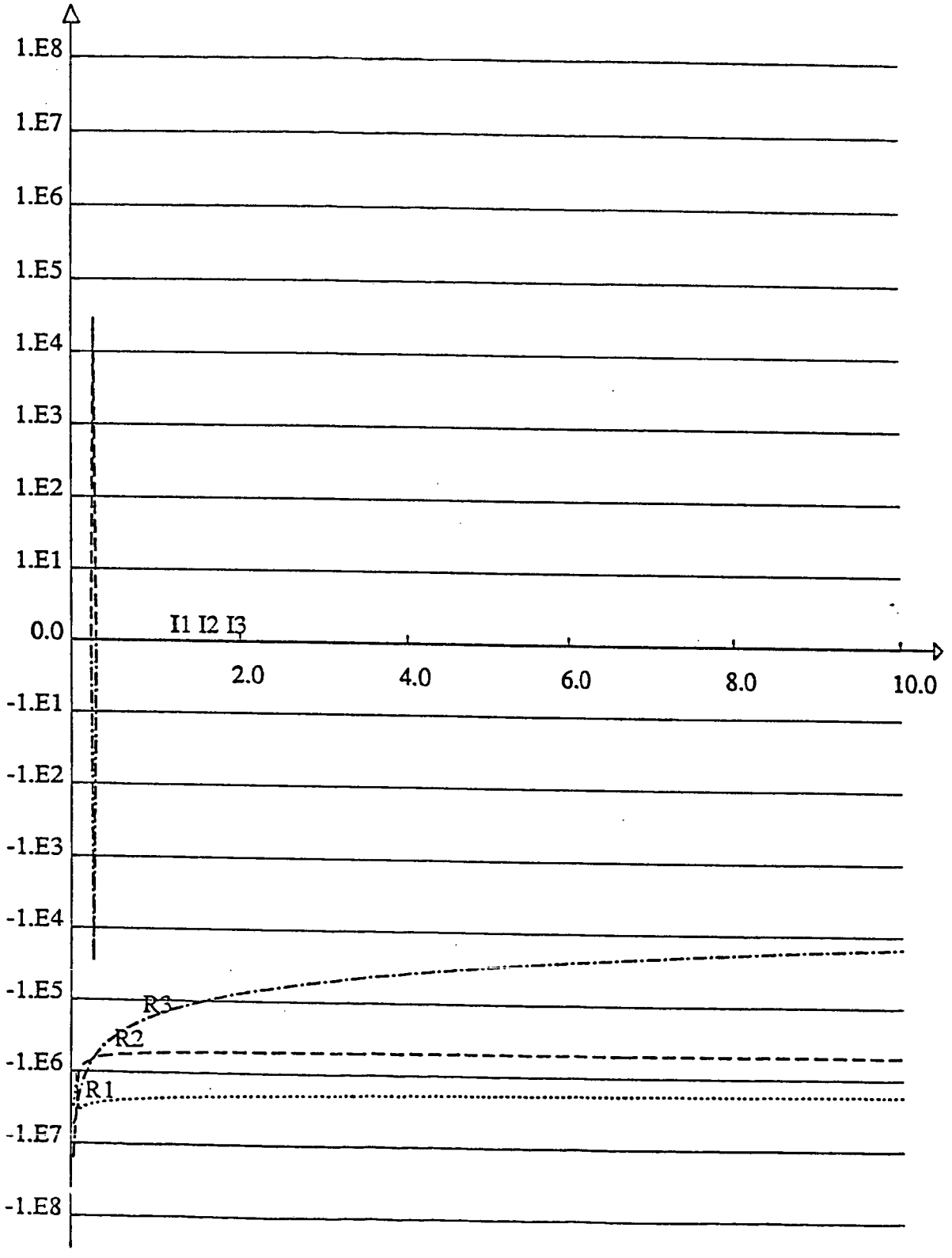

figure 18

Imprimé en France
par
l'Institut National de Recherche en Informatique et en Automatique